

# The environmental history of group and cluster galaxies in a $\Lambda$ CDM Universe

Gabriella De Lucia<sup>1\*</sup>, Simone Weinmann<sup>2</sup>, Bianca M. Poggianti<sup>3</sup>, Alfonso Arag3n-Salamanca<sup>4</sup>, Dennis Zaritsky<sup>5</sup>

<sup>1</sup>INAF - Astronomical Observatory of Trieste, via G.B. Tiepolo 11, I-34143 Trieste, Italy

<sup>2</sup>Leiden Observatory, Leiden University, PO Box 9513, 2300 RA Leiden, the Netherlands

<sup>3</sup>INAF - Astronomical Observatory of Padova, Vicolo dell'Osservatorio 5, Padova I-35122, Italy

<sup>4</sup>School of Physics and Astronomy, The University of Nottingham, University Park, Nottingham NG7 2RD

<sup>5</sup>Steward Observatory, University of Arizona, Tucson, AZ 85721, USA

26 March 2012

## ABSTRACT

We use publicly available galaxy merger trees, obtained applying semi-analytic techniques to a large high resolution cosmological simulation, to study the environmental history of group and cluster galaxies. Our results highlight the existence of an intrinsic *history bias* which makes the nature versus nurture (as well as the mass versus environment) debate inherently ill posed. In particular we show that: (i) surviving massive satellites were accreted later than their less massive counterparts, from more massive haloes; (ii) the mixing of galaxy populations is incomplete during halo assembly, which creates a correlation between the time a galaxy becomes satellite and its present distance from the parent halo centre. The weakest trends are found for the most massive satellites, as a result of efficient dynamical friction and late formation times of massive haloes. A large fraction of the most massive group/cluster members are accreted onto the main progenitor of the final halo as central galaxies, while about half of the galaxies with low and intermediate stellar mass are accreted as satellites. Large fractions of group and cluster galaxies (in particular those of low stellar mass) have therefore been ‘pre-processed’ as satellites of groups with mass  $\sim 10^{13} M_{\odot}$ . To quantify the relevance of hierarchical structure growth on the observed environmental trends, we have considered observational estimates of the passive galaxy fractions, and their variation as a function of halo mass and cluster-centric distance. Comparisons with our theoretical predictions require relatively long times ( $\sim 5 - 7$  Gyr) for the suppression of star formation in group and cluster satellites. It is unclear how such a gentle mode of strangulation can be achieved by simply relaxing the assumption of instantaneous stripping of the hot gas reservoir associated with accreting galaxies, or if the difficulties encountered by recent galaxy formation models in reproducing the observed trends signal a more fundamental problem with the treatment of star formation and feedback in these galaxies.

**Key words:** galaxies: clusters: general – galaxies: evolution – galaxies: formation.

## 1 INTRODUCTION

The observed properties of galaxies have long been known to depend on the ‘environment’ in which they are located. This correlation was quantified by early work showing that galaxy clusters are distinguished by lower fractions of star forming, disc dominated galaxies than regions of ‘average’ density (e.g. Hubble & Humason 1931; Oemler 1974; Dressler 1980). In recent years, observational studies trying to assess

the role of environment on galaxy evolution have received much impetus from the completion of large spectroscopic and photometric surveys at different cosmic epochs (e.g. Kauffmann et al. 2004; Balogh et al. 2004; Cucciati et al. 2006; Cooper et al. 2006, just to mention a few). Despite much effort, however, disentangling the environment(s) and related physical processes that are responsible for the observed trends has proved difficult, and their physical origin is still subject of an active debate.

Much of the argument centres on whether these trends are the end product of physical processes coming into play

\* Email: delucia@oats.inaf.it

only after galaxies have become part of a ‘group’ or of a ‘cluster’ (the *nurture* hypothesis), or whether they are established before these events take place, due to galaxy formation proceeding differently in overdense regions (the *nature* hypothesis). In the current standard paradigm for structure formation, dark matter collapses into haloes in a bottom-up fashion: small objects form first and subsequently merge into progressively larger systems. As structure grows, galaxies join more and more massive systems, therefore experiencing a variety of environments during their lifetimes. In this context, the *nature-nurture debate appears to be ill posed*, as these two elements of galaxy evolution are inevitably and heavily intertwined.

As for the nurture scenario, a variety of physical processes might be effective in suppressing star formation and affecting the morphology of cluster galaxies. Broadly speaking, these can be grouped in two big families: (i) interactions with other cluster members and/or with the cluster potential, and (ii) interactions with the hot gas that permeates massive galaxy systems. The influence of these physical processes and their characteristic time-scales have been studied using detailed numerical simulations (for a review, see e.g. De Lucia 2011). This work has shown, for example, that the pressure experienced by galaxies travelling through a dense intra-cluster medium (*ram-pressure*) can be effective in removing the galaxy interstellar-medium, thereby suppressing subsequent episodes of star formation (Gunn & Gott 1972). Ram-pressure is expected to be more important at the centre of massive clusters, because of the large relative velocities and higher densities of the intra-cluster medium. Galaxies orbiting in massive clusters also experience repeated fast encounters with other cluster members. The cumulative effect of these encounters (*harassment*) can drive a strong internal dynamical response, leading for example to the transformation of spiral galaxies into dwarf spheroidals (Farouki & Shapiro 1981; Moore et al. 1998).

As discussed above, however, these physical processes should be coupled with a *history bias* that is integral part of the hierarchical structure formation. Until about one decade ago, this effect was believed to play a minor role: early numerical work found no dependence of the clustering of dark matter haloes on their properties, such as concentration or formation time<sup>1</sup> (Lemson & Kauffmann 1999; Percival et al. 2003). Taking advantage of high resolution simulations of structure formation, however, recent studies have demonstrated that halo properties like concentration, spin, shape, and internal angular momentum exhibit clear environmental dependencies (e.g. Avila-Reese et al. 2005). Haloes in *over-dense* regions form statistically earlier and merge more rapidly than haloes in regions of the Universe of *average* density (Gao et al. 2005; Maulbetsch et al. 2007). This differential evolution is bound to leave an ‘imprint’ on the observable properties of galaxies that inhabit different regions at any cosmic epoch. In this context, a crucial missing ingredient for a correct interpretation of the observed environmental trends is represented by a detailed characterization and quantification of the *environmental history* of group and cluster galaxies.

A few recent studies have touched this issue. Brüggén & De Lucia (2008) combined semi-analytic models of galaxy formation with analytic models for the gas distribution in clusters to study the ram-pressure histories of present day cluster galaxies. They showed that virtually all cluster galaxies suffered episodes of ram-pressure during their life-time, and argued that this physical process might have a significant role in shaping the observed properties of the entire cluster galaxy population. More recently, Berrier et al. (2009) and McGee et al. (2009) have studied the accretion history of galaxies onto clusters with the aim to quantify the relevance of pre-processing in galaxy groups. These two studies make use of different methods, and reach different conclusions. In the following, we will discuss findings from these studies in more detail, and will compare them with our results.

In this study, we adopt an approach similar to that employed by McGee et al. (2009). In particular, we take advantage of publicly available galaxy merger trees, obtained by applying semi-analytic techniques to a large high resolution cosmological simulation. These merger trees are analysed in order to study the history of the environments that galaxies have experienced during their lifetime, as a function of the parent halo mass at present day, and as a function of present day galaxy stellar mass. The layout of the paper is as follows: in Section 2, we provide a brief description of the models used in our study, and describe the method and definitions adopted. In Section 3, we characterize the history of galaxies in terms of their parent halo mass, and define times that should play a relevant role in their evolution. In Section 4, we discuss the expected trends due to the environmental history for galaxies of different stellar mass. We also compare these expectations with observational estimates of the fraction of red and passive galaxies as a function of parent halo mass, galaxy stellar mass, and cluster-centric distance. Finally, we discuss our results in Section 5, and summarize our conclusions in Section 6.

## 2 THE GALAXY FORMATION MODELS

In this study, we take advantage of the publicly available catalogues from the galaxy formation model presented in De Lucia & Blaizot (2007), and applied to the Millennium Simulation (Springel et al. 2005). This simulation follows  $N = 2160^3$  particles of mass  $8.6 \times 10^8 h^{-1} M_{\odot}$  within a co-moving box of  $500 h^{-1} \text{Mpc}$  on a side. It is based on a  $\Lambda\text{CDM}$  model with parameters  $\Omega_m = 0.25$ ,  $\Omega_b = 0.045$ ,  $h = 0.73$ ,  $\Omega_{\Lambda} = 0.75$ ,  $n = 1$ , and  $\sigma_8 = 0.9$ , where the Hubble constant is parameterised as  $H_0 = 100 h \text{ km s}^{-1} \text{Mpc}^{-1}$ . The simulation outputs were used to construct merger trees of all gravitationally self-bound dark matter subhaloes down to 20 particles, which corresponds to a mass of  $1.7 \times 10^{10} h^{-1} M_{\odot}$ . These merger trees represent the basic input needed for the semi-analytic model described in De Lucia & Blaizot (2007).

Down to the resolution limit of the Millennium Simulation, this model has been shown to provide a reasonable agreement with a large variety of observational data, both in the local Universe and at high redshift. It is, however, not without problems. In particular, the predicted galaxy stellar mass function exhibits an excess of low-to-intermediate mass

<sup>1</sup> This is usually defined as the time when half of the final mass of the halo is first assembled in a single object.

galaxies at all redshifts, the fraction of red galaxies among low mass galaxies is too high compared to observational data, and the model over-predicts the clustering signal of faint galaxies (e.g. Weinmann et al. 2006; Wang et al. 2008; Fontanot et al. 2009). It is important to note that these ‘failures’ are not specific of the particular model adopted in this study. Rather, they appear to be common to most (all) models that have been published recently, and have likely related causes. No satisfactory explanation and/or solution has been found yet to solve all of the problems mentioned above (for recent attempts, see e.g. Guo et al. 2011 and Wang, Weinmann & Neistein 2011).

The model used in this study neglects environmental physical processes such as ram-pressure and harassment, but assumes that when galaxies are accreted onto a more massive system, the associated hot gas reservoir is stripped instantaneously. This induces a very rapid decline of the star formation histories of satellite galaxies, and contributes to create an excess of red and passive galaxies with respect to the observations (e.g. Wang et al. 2007). In recent studies, a more gradual stripping of the hot gas reservoir has been assumed (Kang & van den Bosch 2008; Font et al. 2008; Weinmann et al. 2010; Guo et al. 2011), following results from numerical simulations (McCarthy et al. 2008, but see also Saro et al. 2010). Albeit improved, the agreement with observational measurements is far from satisfactory (e.g. Guo et al. 2011; Weinmann et al. 2011). In this study, we will make limited use of the physical properties of galaxies as predicted by the model. In particular, we will use only the predicted galaxy stellar mass, and we will focus on the resulting galaxy merger trees and their dependence on the parent halo mass. In the following, we will focus on haloes selected from the box of the simulation corresponding to  $z=0$ , with mass larger than  $\sim 10^{13} M_{\odot}$ . The halo mass is computed from the  $N$ -body simulation, as the mass within a sphere enclosing a mean overdensity that is equal to 200 times the critical density of the Universe ( $M_{200}$ ). At the resolution of the Millennium Simulation, haloes with  $M_{200} \sim 10^{13} M_{\odot}$  contain on average about 15 galaxies within the virial radius ( $R_{200}$  in this study), with stellar mass larger than  $\gtrsim 10^9 M_{\odot}$ . To investigate trends as a function of halo mass, we have randomly selected fifteen haloes in each of the following mass bins:  $\sim 10^{13}$ ,  $\sim 5 \times 10^{13}$ ,  $10^{14}$ , and  $\sim 5 \times 10^{14} M_{\odot}$ . These haloes contain 9201 satellite galaxies within their virial radii, that represent the basic sample of our analysis. 6929 of these satellites have present day stellar mass between  $10^9$  and  $10^{10} M_{\odot}$ , 2081 have mass between  $10^{10}$  and  $10^{11} M_{\odot}$ , and only 191 of them have stellar mass larger than  $10^{11} M_{\odot}$ .

In order to clarify the method and the definitions that we have adopted and that we will use in the following, we show in Figure 1 an example of a galaxy merger tree. The galaxy considered is shown at the top of the plot, and all its progenitors (and their histories) are shown going backward in time. The size of the symbols scales with the galaxy stellar mass, while different colours are used for central galaxies (shown in black), satellite galaxies associated with a distinct dark matter substructure (green), and satellite galaxies whose parent dark matter subhaloes have been stripped below the resolution of the simulation (these are shown in red). We note that only central galaxies are fuelled by cooling flows in our model. The leftmost branch in Figure 1 is

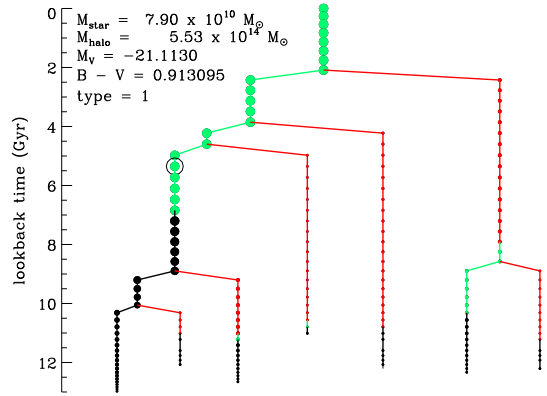


**Figure 1.** Example merger tree for a galaxy of stellar mass  $\sim 8 \times 10^{10} M_{\odot}$ , residing in a halo of mass  $\sim 5.5 \times 10^{14} M_{\odot}$ . The size of the symbols scales with the galaxy stellar mass while different colours are used for central galaxies (black), satellite galaxies associated with distinct dark matter subhaloes (green), and satellites whose parent substructures were stripped below the resolution of the simulation (red). The empty black circle at lookback time  $\sim 5.5$  Gyr corresponds to the lookback time before the galaxy is accreted onto the main progenitor of the final halo.

obtained by connecting the galaxy to its most massive progenitor (often referred to as the *main progenitor*), at each node of the tree.

In the following, when tracing the history of our model galaxies, we will effectively refer to the main progenitor of the galaxy at each time. In addition, we define two different *characteristic times*: (i) the lookback time before a galaxy becomes satellite of a larger halo, and (ii) the lookback time before the galaxy is accreted onto the main progenitor of the final halo. In the following, we will often refer to the former characteristic time as  $t_{\text{sat}}$  or the time when *the galaxy becomes a satellite*, and to the latter as  $t_{\text{halo}}$  or the time when *the galaxy is accreted onto the final group/cluster*. In the example shown in Figure 1,  $t_{\text{sat}}$  corresponds to the last time when the colour of the main progenitor is black before becoming green ( $\sim 7$  Gyr), while  $t_{\text{halo}}$  is marked by an empty black symbol ( $\sim 5.5$  Gyr for the example considered). As we will discuss in detail in the following, the adoption of different characteristic times is largely responsible for the different conclusions reached by Berrier et al. (2009) and McGee et al. (2009).

By construction, the difference between  $t_{\text{sat}}$  and  $t_{\text{halo}}$  has to be positive, or zero. Figure 2 shows the distribution of  $t_{\text{sat}} - t_{\text{halo}}$ , for galaxies of different stellar mass. As the trends are similar for haloes of different mass, we have considered here all galaxies in all haloes analysed for this study. The figure shows that for  $\sim 40$  to  $\sim 60$  per cent of the galaxies, the two events considered happen at the same time. For the remaining galaxies, these two events can differ by up to  $\sim 8$  Gyr. A larger fraction of the most massive galaxies in our sample are accreted as centrals and, for these galaxies, the difference between the two events considered is on average smaller than for less massive galaxies. This results from the combination of different factors. There is a strong cor-

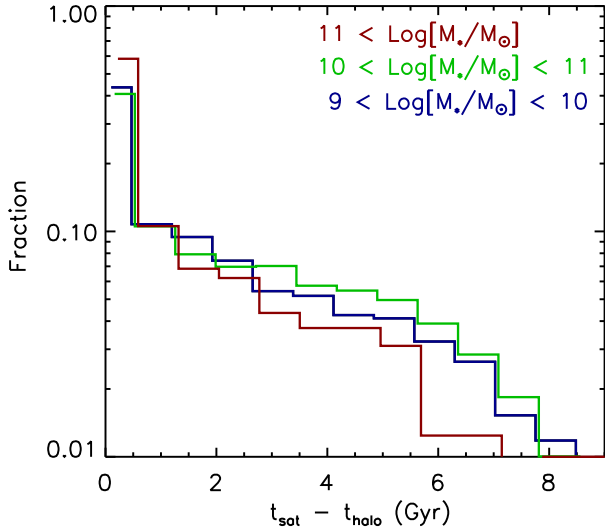


**Figure 2.** Distribution of the difference between the lookback time corresponding to the event of being accreted onto another system (i.e. becoming a satellite), and that corresponding to the accretion onto the final group/cluster (see text for details). Different colours correspond to galaxies of different present day stellar mass, as indicated in the legend.

relation between the stellar mass of central galaxies and the parent halo mass, and massive haloes form relatively late in hierarchical cosmologies. So the most massive galaxies can only be satellites of very massive haloes: the main progenitor of the parent halo has to be already quite massive in order to accrete a second system that is also large enough to contain a massive galaxy. In addition, massive galaxies that were accreted early on during the history of the parent halo, will be rapidly dragged closer to the inner regions by dynamical friction, and eventually merge with the central galaxy of the final halo. Therefore, these galaxies will not appear in our sample that only contains satellite galaxies surviving at redshift zero.

Before studying the history of the environments of our model galaxies, it is interesting to analyse their present day distribution as a function of the parent halo mass, and how it varies as a function of cosmic time. Figure 3 shows the differential (top panels) and cumulative (bottom panel) distribution of galaxies for three different galaxy stellar mass thresholds (increasing from left to right columns). These have been obtained by using the entire volume of the Millennium Simulation, and all galaxies with stellar mass  $\gtrsim 10^9 M_\odot$ . Different line styles correspond to different cosmic epochs (solid is for present day, dotted for  $z \sim 0.5$ , and dashed for  $z \sim 1$ ). Each distribution has been normalized to the total number of galaxies above the stellar mass limit indicated in the legend. Note that the cumulative distributions in the bottom left and middle panels do not reach unity at the lowest halo mass limit shown:  $\sim 55$  per cent of the galaxies with stellar mass larger  $\gtrsim 10^9 M_\odot$  reside today in haloes with mass  $< 10^{12} M_\odot$ . For galaxies more massive than  $\sim 10^{10} M_\odot$ , the corresponding fraction drops to  $\sim 40$  per cent, and it becomes zero for galaxies more massive than  $\sim 10^{11} M_\odot$ .

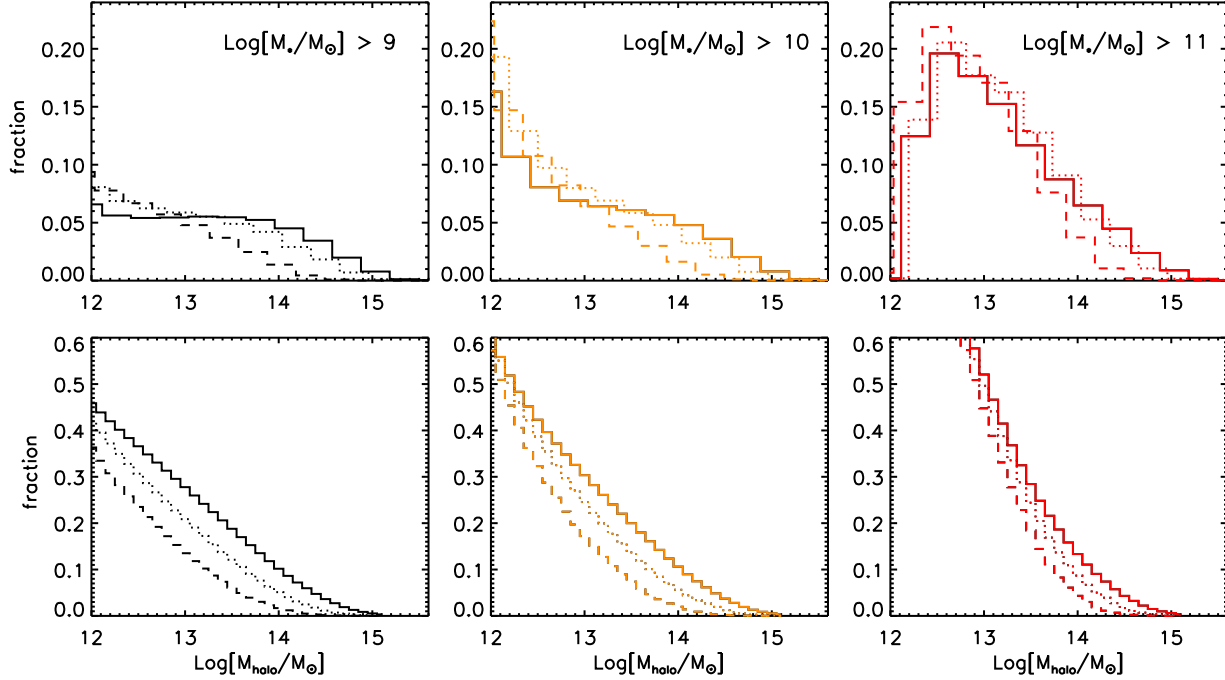
If one defines as *clusters* all haloes more massive than  $\sim 10^{14} M_\odot$ , the figure shows that only about 10 per cent of the cosmic galaxy population resides in clusters at present, and that this is approximately independent of the galaxy stellar mass threshold considered. As expected, this fraction decreases at higher redshift, as massive clusters form relatively late. The figure also shows that more massive galaxies tend to reside in more massive haloes: about 50 per cent of the galaxies with stellar mass  $\gtrsim 10^{11} M_\odot$  reside in haloes more massive than  $\gtrsim 10^{13} M_\odot$ , that are sometimes referred to as *groups* in the literature<sup>2</sup>. When considering all galaxies with stellar mass  $\gtrsim 10^{10} M_\odot$ , however, this fraction drops to only about 30 per cent at the present day. It is even lower for lower stellar mass limits. Therefore, it is not generally true that ‘most galaxies reside in groups’, if by groups one refers to haloes with mass  $\gtrsim 10^{13} M_\odot$ . As just discussed, this statement depends significantly on the stellar mass limit of the observed sample. We stress that the definitions adopted in this paper are theoretical ones, and that they do not necessarily always represent a good proxy for observational definitions. In this paper, we will work in this ‘theory space’, and use the mass of the parent halo (specifically,  $M_{200}$ ) as a proxy for the environment. In future work, we plan to extend our analysis beyond the virial radius, and to use environmental definitions that are closer to those commonly adopted in the literature.

### 3 THE HISTORY OF GROUP AND CLUSTER GALAXIES

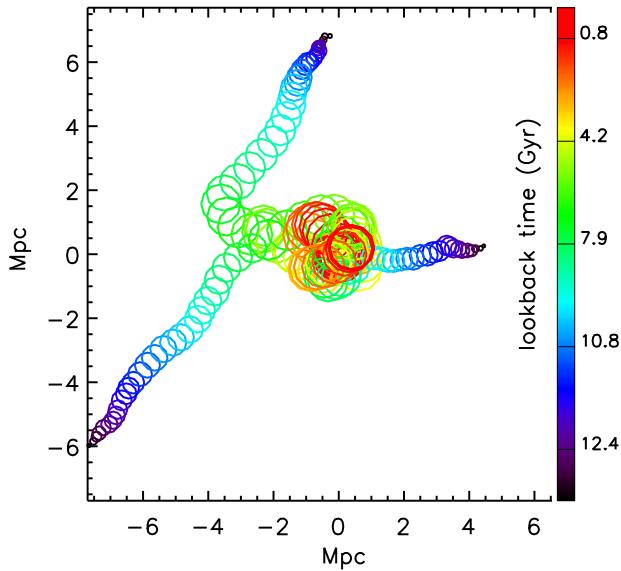
In order to study the environmental history of our model satellite galaxies, we have traced back their histories and stored the values of their parent halo mass at all times. In addition, for each galaxy, we have computed the time when it becomes a satellite, and the time when it is accreted onto the main progenitor of the final halo, and stored the values of the parent halo mass corresponding at these times. In the following, we will refer to the value of the parent halo mass at  $t_{\text{sat}}$  as  $M_{\text{halo}}(\text{sat})$ , and to the corresponding value at  $t_{\text{halo}}$  as  $M_{\text{halo}}(\text{halo})$ .

Figure 4 shows the projected comoving trajectories of three cluster galaxies, re-centred with respect to the positions of the main progenitor of the final halo at each time. The galaxies have been selected randomly between the satellites of haloes with mass  $\sim 10^{14} M_\odot$ , and with present stellar mass  $\gtrsim 10^{11} M_\odot$ . The progenitors of these galaxies come from extended regions around the main progenitor of the final halo, and their parent halo mass (encoded in the size of the symbols) increases progressively as the galaxies get closer. Figure 5 shows the mean evolution of the stellar mass (dashed lines) and parent halo mass (solid lines), computed considering all satellites of 15 haloes with mass  $\sim 10^{14} M_\odot$  (qualitatively, these results do not change significantly when considering different ranges of parent halo mass). The mean evolution of the galaxy stellar mass is very similar in the three mass bins considered. The evolution of the parent halo

<sup>2</sup> Note that the Local Group, with an estimated mass of  $5 \times 10^{12} M_\odot$  (Li & White 2008), would not be classified as a group according to this definition.



**Figure 3.** Differential (top panels) and cumulative (bottom panels) distributions of galaxies as a function of their parent halo mass. Different columns correspond to different galaxy stellar mass thresholds, as indicated in the legend. Different line styles correspond to different cosmic epochs (solid, dotted and dashed lines are used for  $z \sim 0$ , 0.5, and 1, respectively). Each distribution is normalized to the total number of galaxies above the stellar mass limit considered (without dividing by the bin size).



**Figure 4.** Projected (comoving) positions of the main progenitors of three cluster galaxies, selected randomly between the satellites with stellar mass  $\gtrsim 10^{11} M_{\odot}$ , residing in haloes with mass  $\sim 10^{14} M_{\odot}$ . Coordinates are re-centred with respect to the positions of the main progenitor of the final cluster. The size of the symbols scales with the parent halo mass, while the colours encode the lookback time.

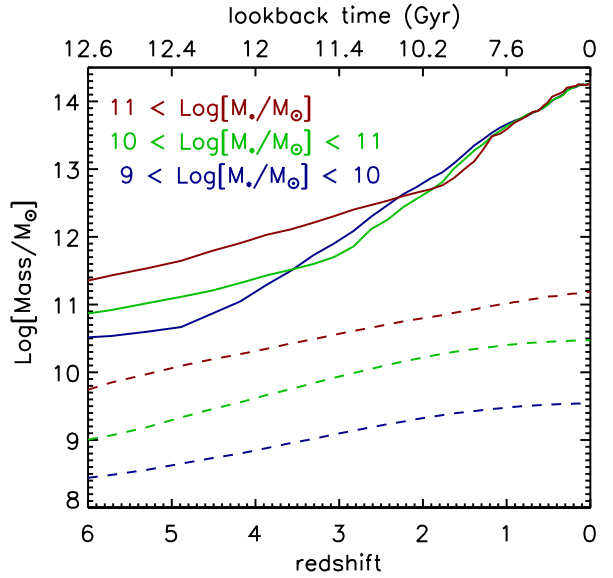


**Figure 5.** Mean evolution of the galaxy stellar mass (dashed lines), and of the parent halo mass (solid lines). These have been computed by averaging the evolution of all satellites of haloes with mass  $\sim 10^{14} M_{\odot}$ . Different colours correspond to galaxies of different present day stellar mass, as indicated in the legend.

masses (solid lines) shows clearly that more massive galaxies are sitting on average in more massive haloes for most of their evolution (before starting being accreted onto the final

haloes). The difference in mass is, however, not large. In addition, Figure 5 also shows that the most massive galaxies surviving at redshift zero fell onto the main progenitor of the final cluster later than their less massive counterparts: all lines superimpose when galaxies are in the same halo, and for the most massive galaxies this happens only at  $z \sim 1$ .

It is very instructive to look at some properties of group/cluster satellites at the characteristic times defined above. The left panel of Figure 6 shows the time since the galaxy became a satellite as a function of the corresponding parent halo mass, for all galaxies residing in a single cluster of mass  $M \sim 5 \times 10^{14} M_\odot$  at  $z = 0$ . The solid line shows the mass accretion history of the parent cluster, while the size of the symbols scales with the present day galaxy stellar mass, as indicated in the legend in the right panel. The figure shows that cluster members with low stellar mass become satellites (are accreted onto more massive haloes) at all times, while the (few) most massive galaxies that survive as satellites at redshift zero tend to become satellites later compared to the overall cluster galaxy population. As discussed in the previous section, this is expected in a hierarchical cosmology.

Since the number of galaxies in a halo increases with halo mass, those galaxies that became satellites when sitting in massive systems also have larger numbers of companion galaxies at that time, as shown in the right panel of Figure 6. Interestingly, the bottom right corners of both panels in Figure 6 appear to be rather ‘empty’. The mass of the cluster considered in our particular example grows significantly down to a lookback times  $\sim 4$  Gyr (that corresponds to  $z \sim 0.4$ ), through the accretion of few relatively massive structures. At lower redshift, the mass growth of the parent halo is not significant, and it is mainly driven by the accretion of small haloes and diffuse material. Most of the galaxies that become satellites at lookback times lower than  $\sim 4$  Gyr are accreted directly onto the main progenitor of the final cluster, and have low stellar mass. As we will see below, these results hold for the statistical sample considered in this study. It is interesting that this regime of ‘slow mass growth’ for the parent haloes coincides with the cosmic epoch that witnesses the most striking transformations for the cluster galaxy population, both in terms of their star formation activity and morphological mix (e.g. Butcher & Oemler 1984; Desai et al. 2007).

Figure 7 shows the distributions of the times when group/cluster members become satellite galaxies (top left panel), of the times when the galaxies are accreted onto the final halo (bottom left panel), and the corresponding distributions of parent halo mass (right panels). As there is no significant trend as a function of final halo mass, we have stacked together all haloes in our sample. The top left panel of Figure 7 shows that cluster/group members became satellite galaxies over a wide range of lookback times. The distributions for low and intermediate mass galaxies exhibit a peak at very early epochs ( $\sim 10$  Gyr), while the distribution obtained for the most massive galaxies is peaked at later times, with most of them becoming satellite between 4 and 9 Gyr ago.

The top right panel of Figure 7 shows a strong correlation (albeit with a relatively large scatter) between the present day galaxy stellar mass and the parent halo mass at  $t_{\text{sat}}$ . This reflects the strong correlation between halo mass

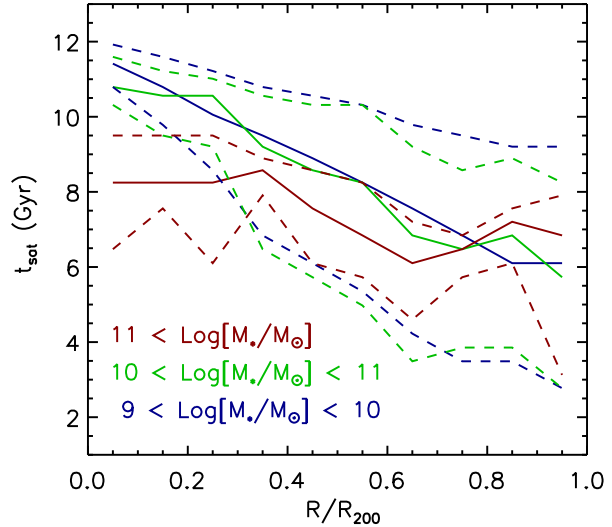


**Figure 8.** Median (solid lines) and percentiles (25th and 75th) of the lookback times since cluster galaxies became satellites, as a function of their present day (three-dimensional) distance from the cluster centre. This has been obtained by stacking all haloes with mass  $\sim 5 \times 10^{14} M_\odot$  in our sample. Different colours refer to different galaxy stellar mass bins, as indicated in the legend.

and galaxy stellar mass for central galaxies. This correlation is preserved for satellite galaxies because their stellar mass does not increase significantly after being accreted, as their star formation is efficiently suppressed over a quite short time-scale in our model. The distribution of parent halo masses found for the most massive galaxies is also the widest, due to the fact that the relation between the galaxy stellar mass and the parent halo mass flattens at high stellar masses. The distributions shown in the top panels of Figure 7 look different when one considers the time when the galaxies were accreted onto the most massive progenitor of the final halo ( $t_{\text{halo}}$ ). These distributions are shown in the bottom panels of Figure 7. Since, as discussed above, the two times considered tend to coincide for the most massive galaxies, the distributions computed for these galaxies are not significantly different. Results are instead different for low and intermediate stellar mass galaxies. A large fraction of these tend to be accreted when they are already satellite galaxies, so that the distributions of  $t_{\text{halo}}$  are shifted towards later cosmic epochs with respect to the corresponding distributions of  $t_{\text{sat}}$ . As a consequence, if one looks at the distribution of halo masses at  $t_{\text{halo}}$ , this is found to be ‘bimodal’ for these galaxies. The peaks at lower halo masses are made up of galaxies that are accreted when they are central galaxies of their own haloes, while the peaks corresponding to larger parent halo masses are populated by galaxies that are accreted as satellites of relatively large systems. In particular, we find that  $\sim 48$  per cent of the galaxies in the lowest stellar mass bin considered were accreted as satellite galaxies. The fraction is slightly lower ( $\sim 43$  per cent) for the intermediate mass bin considered, while it drops to only  $\sim 23$  per cent for the most massive galaxies in our sample.

Substructures that were accreted onto the main progen-



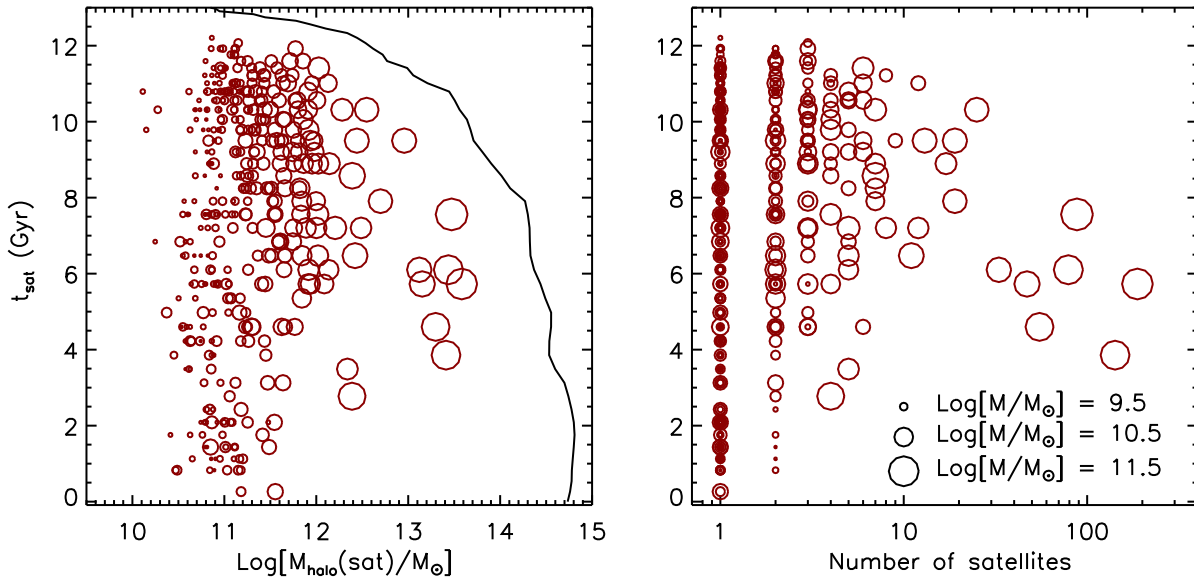


**Figure 6.** Left panel: lookback time corresponding to the event of becoming a satellite galaxy, as a function of the parent halo mass at the same time. Each symbol corresponds to a galaxy, with the symbol size scaling proportionally to the present day stellar mass. The example shown corresponds to a single halo of mass  $M \sim 5 \times 10^{14} M_{\odot}$ , selected at  $z = 0$ . The solid thick line shows the mass evolution of the cluster main progenitor. Right: lookback time corresponding to the event of becoming a satellite as a function of the galaxy’s number of satellites at the same time.

itor of their parent halo at early times had relatively short orbital periods. So these should be located, on average, in the inner regions of the final halo. In addition, these haloes will have suffered from dynamical friction for a longer time with respect to haloes of similar mass but accreted later. These two factors combine to create a strong correlation between the accretion time and the cluster-centric distance of dark matter substructures (Gao et al. 2004). Figure 8 shows that this correlation is also found for cluster galaxies, although with a large scatter. Therefore, a radial dependence of galaxy properties is, at least in part, a natural consequence of the fact that mixing of the galaxy population is incomplete during cluster assembly. The weakest trend is found for the most massive satellites surviving at redshift zero that, as discussed above, were accreted later than their less massive counterparts. The radial trend is stronger for the low and intermediate stellar mass galaxies considered: those that are located closer to the centre have been orbiting as satellite galaxies for about 11 Gyr, while those that are located at the outskirts of the haloes have been satellites for about 6 Gyr on average. As we will discuss in more detail in the following section, the trends shown in Figure 8 can be combined with the observed fractions of red/passive galaxies as a function of cluster-centric distance to put constraints on the physical processes (and corresponding timescales) responsible for the suppression of star formation activity in group and cluster galaxies.

A figure similar to our Figure 8 has been shown in Weinmann, van den Bosch & Pasquali (2011) who took advantage of the same simulated galaxy catalogues but used a cluster sample selected mimicking a specific observational data-set, and plotted results as a function of the projected cluster-centric radius. Similar findings have also been discussed in a recent work by Smith et al. (2012). These au-

thors have based their analysis on publicly available catalogues from the model presented in Font et al. (2008, also based on the Millennium Simulation). In particular, they have selected all galaxies residing in the five most massive haloes in the simulation, and studied how various characteristic epochs of the evolution of model galaxies relate to their present day projected distance from the cluster centre. The results by Smith et al. (2012) are in very good agreement with those by Weinmann et al. (2011) and with ours, confirming that these findings are not significantly dependent on the particular model used, but mainly driven by structure formation.

#### 4 HISTORY BIAS

The results shown in the previous section demonstrate that the galaxy population of groups and clusters is characterized by a variety of accretion histories, and that these are strongly dependent on the final galaxy stellar mass. In this section, we will discuss how the results found above can influence the observed environmental trends. In particular, we will focus on two observables: the fraction of passive/red galaxies that reside in haloes of different mass, and its variation as a function of the cluster-centric distance.

Figure 9 shows the fraction of galaxies that spent a time longer than that given on the x-axis in haloes with mass larger than  $10^{12}$  (cyan),  $10^{13}$  (green), and  $10^{14} M_{\odot}$  (orange). In this Figure, each solid thin line corresponds to a different halo, while the thick solid lines show the mean obtained for the 15 haloes considered in each sample. As a consequence of the hierarchical structure formation, the fraction of galaxies that have resided in haloes more massive than  $M_{\text{halo}}$  for a time longer than  $T_{\text{halo}}$  decreases when considering both more

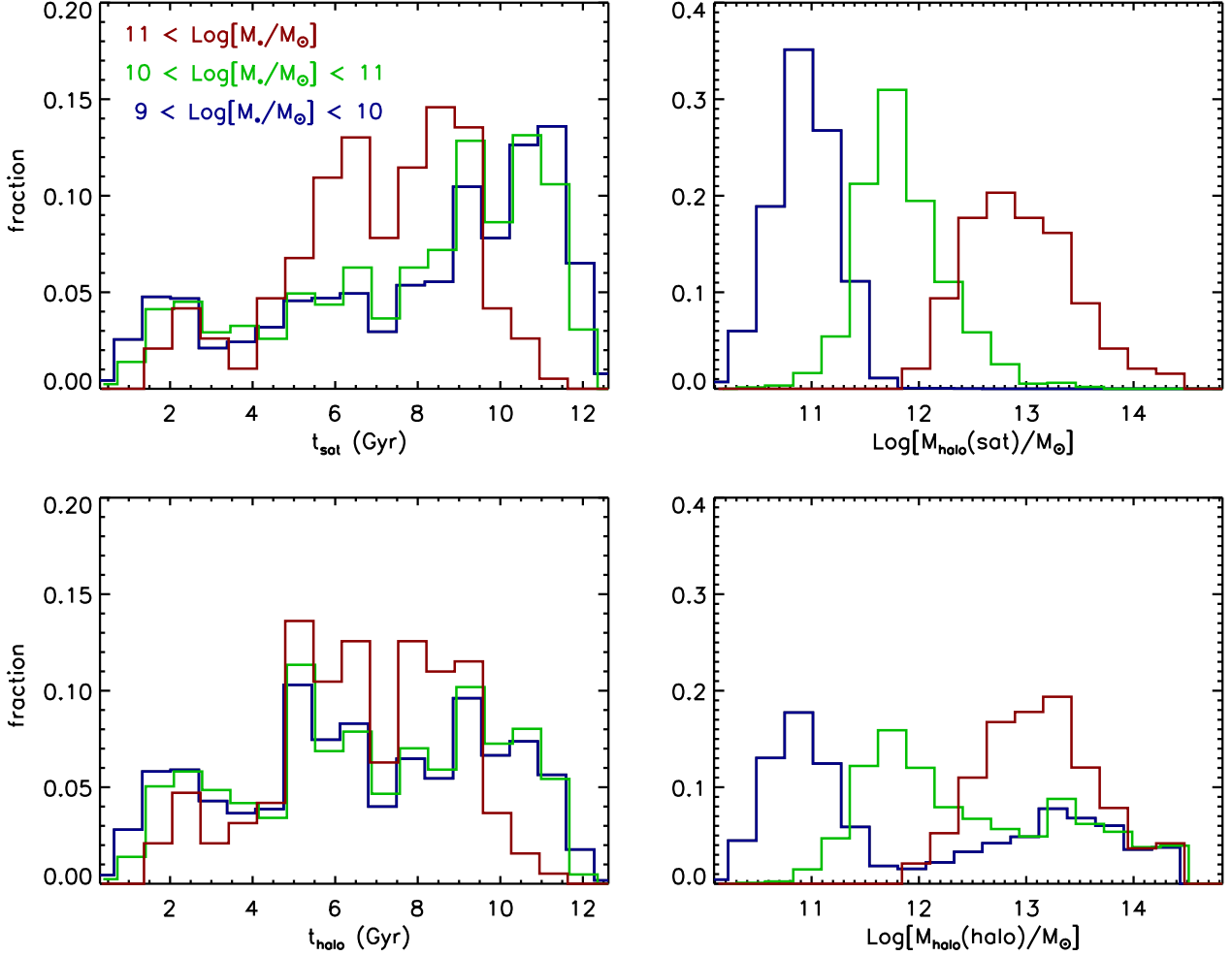


**Figure 7.** Distributions of the times when group/cluster members become satellite galaxies (top left panel), and of the times when the galaxies are accreted onto the main progenitor of the final halo (bottom left panel). The right panels show the corresponding distributions of parent halo masses. The distributions shown have been computed using all haloes selected at  $z = 0$ . Different colours correspond to different present day galaxy stellar mass, as indicated in the legend.

massive haloes and longer times. So it is not surprising that the thick green lines are always below the thick blue lines, and that these are always above the red lines. Interestingly, the figure shows a relatively large halo-to-halo scatter: e.g. focusing on the most massive haloes in our sample, the fraction of galaxies that have spent more than 6 Gyr in haloes more massive than  $10^{14} M_{\odot}$  varies between  $\sim 20$  per cent and  $\sim 80$  per cent. If the time spent in a more massive halo can be related to the star formation activity (or lack thereof) of a galaxy, this halo-to-halo scatter can be linked to the different fractions of passive galaxies measured in different clusters (e.g. in the nearby Coma and Virgo clusters, Weinmann et al. 2011) and, more in general, to the scatter measured for some properties of the galaxy populations of groups and clusters (see e.g. De Lucia, Fontanot & Wilman 2012). Interestingly, the observed fraction of red/passive galaxies does indeed show a large halo-to-halo scatter, that appears to increase at lower halo masses (Poggianti et al. 2006; Balogh & McGee 2010). It should be noted, however, that observational uncertainties are usually much larger for

lower mass systems. In addition, as we will show in the next sections, the fraction of passive galaxies increases only weakly as a function of halo mass, and is larger than  $\sim 0.4$  in haloes of mass  $\sim 10^{13} M_{\odot}$ . Taken at face value, these results favour a value for  $M_{\text{halo}}$  (i.e. the halo mass above which star formation starts to decline) lower than  $10^{14} M_{\odot}$  that would produce a too low fraction of passive galaxies in haloes with present day mass  $\sim 5 \times 10^{13} M_{\odot}$  or lower.

We discuss this in more detail in the following subsections, where we investigate how the trends shown in Figure 9 depend on galaxy stellar mass and on the cluster-centric distance, and how the theoretical expectations compare to the estimated fractions of ‘passive’ or ‘red’ group/cluster galaxies.

#### 4.1 Observational data

To constrain our theoretical models, we take advantage of the group catalogue by Yang et al. (2007) complemented with the cluster catalogue by von der Linden et al.



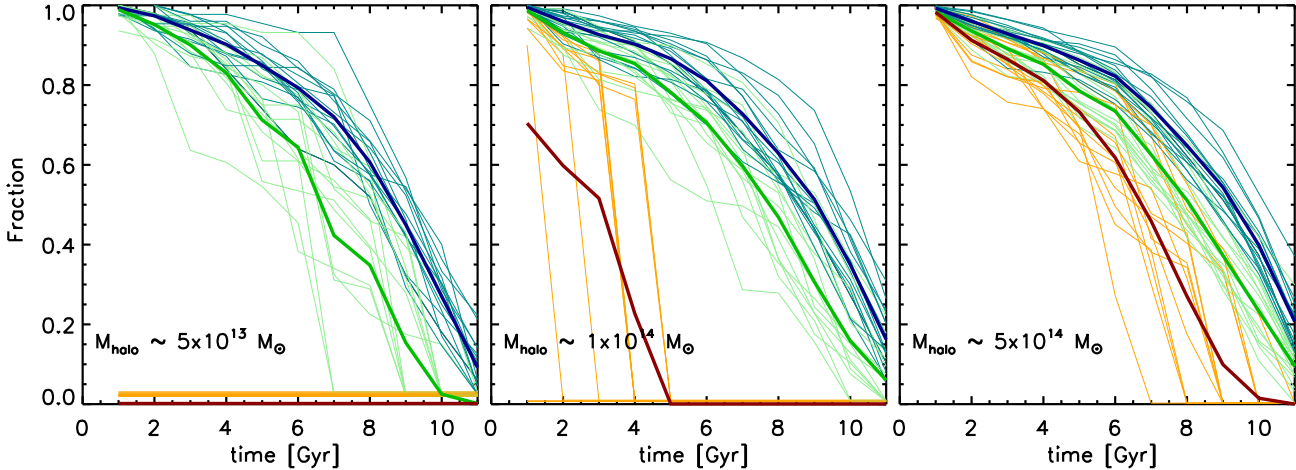


**Figure 9.** Fraction of galaxies that spent a time longer than that given on the x-axis in haloes with mass larger than  $10^{12}$  (blue),  $10^{13}$  (green), and  $10^{14} M_{\odot}$  (orange). Each solid thin line corresponds to a single halo, while the corresponding thick lines represent the mean of the distributions. Different panels correspond to galaxies residing in haloes of different mass today (increasing from left to right), as indicated in the legend.

(2007), both based on DR4. Specifically, we use the sample II of the Yang et al. group catalogue, as described in van den Bosch et al. (2008)<sup>3</sup>. We use only satellite galaxies (as in the theoretical predictions discussed below), and weight results according to the maximum value out to which they can be observed, to account for Malmquist bias. Our sample of satellite galaxies based on the Yang et al. catalogue contains 42363 galaxies residing in haloes with mass larger than  $10^{13} M_{\odot}$ . As for the von der Linden et al. (2007) catalogue, their final sample consists of 625 systems at redshifts between 0.03 and 0.1, with masses between  $\sim 10^{12}$  and  $\sim 10^{15} M_{\odot}$ . In the following, we will consider only the 214 systems more massive than  $\sim 10^{14} M_{\odot}$  from this catalogue.

In addition, we make use of the data catalogues for SDSS DR7 from MPA/JHU to obtain up-to-date estimates for stellar masses and specific star formation rates (SSFRs)<sup>4</sup>. Stellar masses are estimated using fits to the photometry, and are statistically in agreement with the estimates from Kauffmann et al. (2003). The SSFRs are based on those published in Brinchmann et al. (2004), but with several modifications regarding the treatment of dust attenuation and aperture corrections. All details can be found at the reference webpage.

Following Weinmann et al. (2006) and Kimm et al. (2009), we have adopted the following demarcation line between red and blue galaxies:

$$^{0.1}(g-r) = 0.7 - 0.032(^{0.1}M_r - 5 \log h + 16.5) \quad (1)$$

All galaxies with  $\log(\text{SSFR}) < -11$  are classified as passive. As shown by Weinmann et al. (2010), this cut corresponds roughly to the location of the minimum in the bimodal distribution of SSFRs in the observations. For comparison, we have also used alternative estimates of the SS-

FRs based on UV data from the GALEX satellite, as described in McGee et al. (2011). This results in a reduction of the sample size by a factor of about 10, as not all SDSS galaxies have GALEX coverage. The scatter in the observational measurements given below gets larger, but qualitatively results do not change. Therefore, we only show our measurements of passive fractions based on the Brinchmann et al. estimates of the SSFRs.

Finally, the cluster sample is complemented with the datasets for Coma and Virgo that are described in detail in Weinmann et al. (2011). For these datasets, stellar mass estimates are obtained from fits to the photometry, using the SDSS g- and r-band filters, according to the fitting formula by Zibetti, Charlot & Rix (2009).

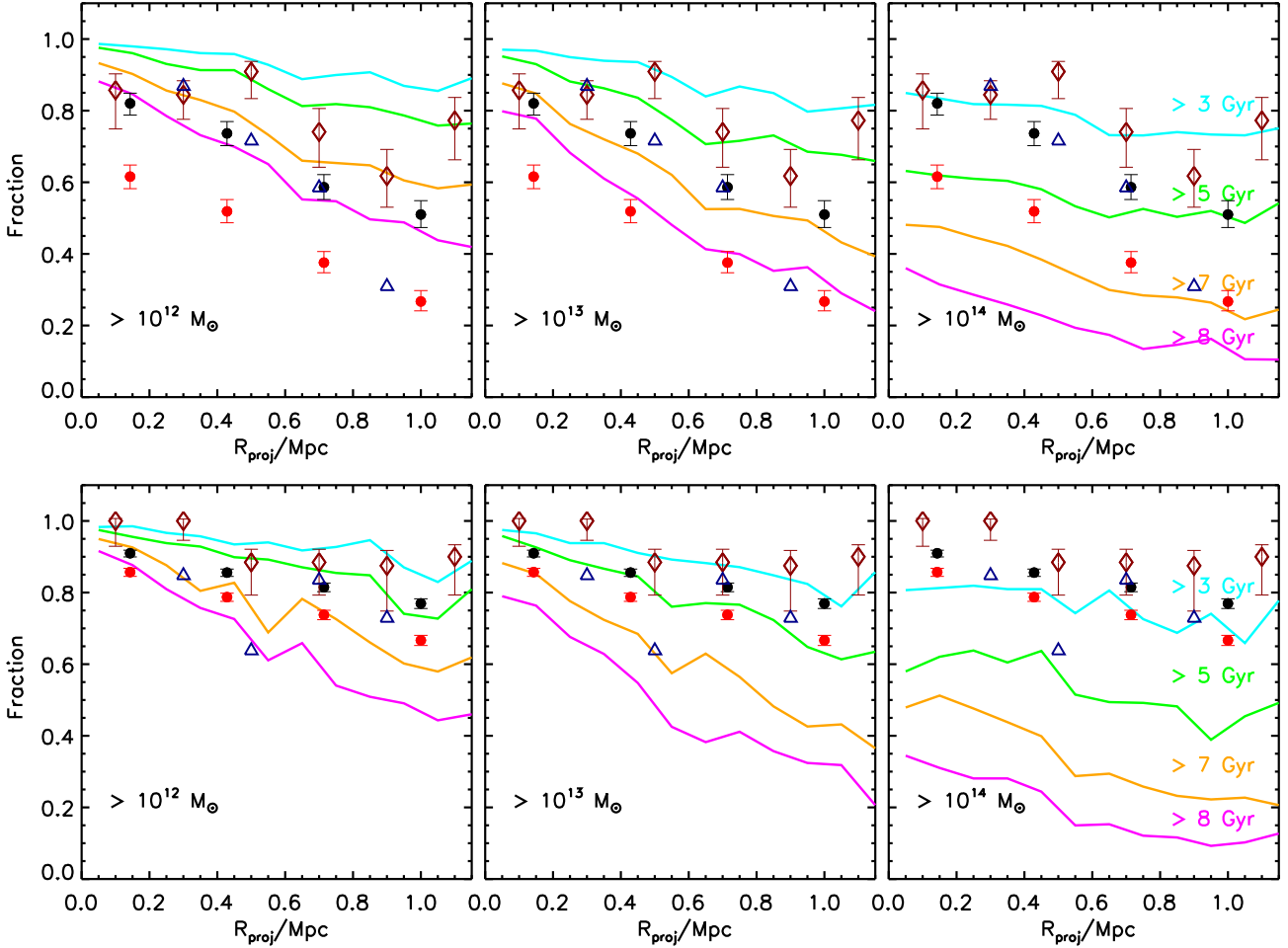
## 4.2 Cluster Radial Dependence

Figure 10 shows the fraction of model galaxies that spent more than 3, 5, 7, and 8 Gyr (lines of different colour) in haloes more massive than the thresholds indicated in the legend of each panel (increasing from left to right). Top and bottom panels are for galaxies with stellar masses in the ranges  $\log(M_{\text{star}}/M_{\odot}) = [9 - 10]$  and  $\log(M_{\text{star}}/M_{\odot}) = [10 - 11]$ , respectively. Theoretical predictions have been obtained averaging all haloes in our sample with mass larger than  $10^{14} M_{\odot}$ , and projecting cluster members on the xy plane. Red diamonds, blue triangles, and black circles show the fractions of red galaxies for the Coma cluster, for the Virgo cluster, and for the cluster catalogue by von der Linden et al. (2007), respectively. Finally, red circles show the fraction of passive galaxies estimated using the catalogue by von der Linden et al. as in Weinmann et al. (2010). Error bars denote confidence intervals corresponding to a probability of 68 per cent ( $1\sigma$ ) from quartiles of the beta distribution (for details on the method, see Cameron 2011).

Interestingly, the red fractions estimated from the cluster sample defined in von der Linden et al. (2007) are in quite good agreement with the red fractions estimated for

<sup>3</sup> The group catalogue is publicly available at: <http://www.astro.umass.edu/~xhyang/Group.html>

<sup>4</sup> The data are publicly available at: <http://www.mpa-garching.mpg.de/SDSS/>.



**Figure 10.** Fraction of model galaxies that spent more than 3, 5, 7, and 8 Gyr (lines of different colour) in haloes more massive than  $10^{12}$  (left panel),  $10^{13}$  (middle panel), and  $10^{14} M_{\odot}$  (right panel). Top panels are for galaxies with stellar mass in the range  $\log(M_{\text{star}}/M_{\odot}) = [9 - 10]$ , while bottom panels are for galaxies in the range  $\log(M_{\text{star}}/M_{\odot}) = [10 - 11]$ . Theoretical predictions have been obtained averaging all haloes in our sample with mass larger than  $10^{14} M_{\odot}$ , and projecting cluster members on the xy plane. Red diamonds and blue triangles show the red fractions for the Coma and Virgo clusters estimated by Weinmann et al. (2011). Black and red circles show the red and passive fractions estimated using the cluster catalogue by von der Linden et al. (2007), respectively. Error bars denote confidence interval estimates measured as described in the text.

the Coma and Virgo clusters. This suggests that neither contamination by background galaxies (this affects at some level the Coma cluster catalogue as it includes photometric members), nor incompleteness due to fiber completeness (which affects the cluster catalogue by von der Linden et al.) influence our results significantly, at least out to a projected radius of  $\sim 1$  Mpc. Both the observed red and passive fractions exhibit a clear dependency on stellar mass: more massive galaxies exhibit a shallower radial trend with respect to their less massive counterparts (compare bottom and top panels of Figure 10), in qualitative agreement with the trends shown in Figure 8. The measured fractions of passive galaxies are generally lower than the fractions of red galaxies, indicating that a fraction of all star forming galaxies are red because dusty. The offset between the red and passive fractions depends on galaxy stellar mass and (albeit weakly) on the projected distance from the cluster centre. In particular, using the results based on the catalogue by von der Linden et al. (2007), we find that a fraction vary-

ing between  $\sim 5$  per cent (at small projected distances) to  $\sim 10$  per cent (at the largest projected distances considered) of the red galaxies are star forming dusty systems in the stellar mass bin  $\log(M_{\text{star}}/M_{\odot}) = [10 - 11]$ . For the lower mass bin considered, the fraction of star forming dusty galaxies gets larger, varying between  $\sim 20$  per cent close to the cluster centre, to  $\sim 24$  per cent at projected distances of  $\sim 1$  Mpc. Our results contradict those by Wolf et al. (2009) who analyse the properties of dusty red galaxies in the A901/2 cluster complex at  $z \sim 0.17$ , and argue that dusty star forming galaxies are rare for  $\log(M_{\text{star}}/M_{\odot}) < 10$  while appearing predominantly in the stellar mass range of  $\log(M_{\text{star}}/M_{\odot}) = [10 - 11]$ . We note, however, that Wolf et al. defined their population of dusty red galaxies differently than done in our study. In particular, Wolf et al. defined red dusty galaxies from a full spectral energy distribution fit to the medium-band photometry of the COMBO-17 survey. This will be more uncertain for faint galaxies (i.e. for

low mass galaxies), a caveat that applies to the passivity criterion used in our study as well.

The theoretical predictions shown in Figure 10 are shallower when considering lower values of  $T_{\text{halo}}$  at fixed  $M_{\text{halo}}$  values, and for the largest values of  $M_{\text{halo}}$  considered (right panels). Again, this is a consequence of hierarchical structure formation: more massive haloes are formed later than their less massive counterparts so that galaxies could spend less time in relatively massive systems. A comparison between theoretical predictions and observational data shows that different combinations of  $T_{\text{halo}}$  and  $M_{\text{halo}}$  can provide a relatively good agreement with the observed radial trends of passive galaxies. For example, for galaxies with stellar mass in the range  $\log(M_{\text{star}}/M_{\odot}) = [9 - 10]$  (upper panels), the observed trend is very close to that obtained when considering galaxies that have been sitting in haloes more massive than  $10^{13} M_{\odot}$  for more than  $\sim 8$  Gyr. A qualitatively good agreement (but with a slope shallower than observed) is obtained when considering galaxies that have been sitting in haloes more massive than  $10^{14} M_{\odot}$  for more than  $\sim 5 - 7$  Gyr. For the more massive bin considered ( $\log(M_{\text{star}}/M_{\odot}) = [10 - 11]$ ), the fraction of passive galaxies has a significantly shallower radial trend. Qualitatively, it is very similar to the trend obtained considering the fraction of galaxies that spent more than  $\sim 7$  Gyr in haloes more massive than  $10^{12} M_{\odot}$ , but also to the trend obtained considering galaxies that spent more than  $\sim 5$  Gyr in haloes more massive than  $10^{13} M_{\odot}$ , or more than  $\sim 3$  Gyr in haloes more massive than  $10^{14} M_{\odot}$ .

### 4.3 Halo mass dependence

Another important and independent constraint to our theoretical predictions is given by the observed fraction of red or passive galaxies as a function of the present day halo mass. Figure 11 compares the fraction of model galaxies that spent more than 3, 5, and 7 Gyr (from left to right panels) in haloes more massive than  $10^{12}$ ,  $10^{13}$ , and  $10^{14} M_{\odot}$  (lines of different style) with observational estimates of red and passive galaxies (top and bottom panels, respectively). To construct the datasets shown in this figure, we have used the DR4 group catalogue by Yang et al. (2007), as detailed above.

Figure 11 shows that both the fraction of red galaxies (top panels) and that of passive galaxies (bottom panels) tend to increase as a function of halo mass. In addition, at fixed halo mass, the fraction of red/passive galaxies is larger for more massive galaxies. The results obtained are in good agreement with those presented in Kimm et al. (2009). As noted above, the fraction of passive galaxies is generally lower than that of red galaxies. In particular, we find that about 16 per cent of the galaxies are red but star forming for the lowest galaxy stellar mass bin considered ( $\log(M_{\text{star}}/M_{\odot}) \sim 9.75$ ). The fraction reduces to about 5 per cent for the largest stellar mass bin considered ( $\log(M_{\text{star}}/M_{\odot}) \sim 11.25$ ): i.e. a larger fraction of red massive galaxies are truly passive, while for less massive galaxies the fraction of star forming but dusty (and therefore red) objects increases. This is in agreement with what discussed about Figure 10, and in contrast with results from Wolf et al. (2009).

In our models, more than 90 per cent of the galaxies with stellar mass larger than  $\log(M_{\text{star}}/M_{\odot}) \sim 9.75$  have

spent more than 3 Gyr in haloes more massive than  $10^{12} M_{\odot}$  (dotted lines in the left panels of Figure 11). When considering longer times (middle and right panels) the fractions decrease, and one can see some dependency on the galaxy stellar mass (larger fractions are obtained for more massive galaxies), in particular for the longest times considered. The fractions of galaxies that have spent equal time in more massive haloes are lower, as a natural consequence of hierarchical structure formation. In particular, our model predicts that only about 60 per cent of the galaxies in the most massive haloes considered in our sample have spent more than 7 Gyr in haloes more massive than  $10^{13} M_{\odot}$  (dashed lines in right panels). The fraction decreases rapidly for less massive haloes. For the most massive galaxies considered (red symbols), the observed passive fractions are in quite nice agreement with the estimated fractions of galaxies that spent more than 5 Gyr in haloes more massive than  $10^{13} M_{\odot}$ . For less massive galaxies, longer times seem to work better (compare cyan lines and points in the bottom middle and right panels of Figure 11).

### 4.4 Central quenching and Satellite quenching

Putting together both the estimated fractions of passive galaxies as a function of halo mass and those as a function of cluster-centric distance, there seems to be a rough timescale/halo mass combination that gives results in quite good agreement with observational measurements:  $M_{\text{halo}} \sim 10^{13} M_{\odot}$  and  $T_{\text{halo}} \sim 5 - 7$  Gyr is needed for a galaxy to be quenched with close to 100 per cent probability, with a tendency for slightly longer timescales and slightly larger halo masses for lower stellar mass galaxies. However, the interpretation of the last two figures shown is not trivial because one has to consider that there is a continuous evolution of the halo mass hosting the galaxies that end up in a group/cluster. In addition, it is necessary to account for galaxies that become passive because of ‘internal’ physical processes (*central-quenching*), rather than for ‘environmental’ processes (*satellite quenching*).

The importance of central-quenching can be estimated by considering the fraction of red/passive central galaxies. Figure 3 by Kimm et al. (2009) shows how this fraction varies as a function of the galaxy stellar mass. Virtually all central galaxies in the first stellar mass bin considered in our study,  $\log(M_{\text{star}}/M_{\odot}) = [9.5 - 10]$ , are active. For the larger stellar mass bins that we have considered in Figure 11, the fraction of passive central galaxies increases to  $\sim 10 - 20$  per cent for the bin  $\log(M_{\text{star}}/M_{\odot}) = [10 - 10.5]$ , and to  $\sim 40 - 50$  per cent for the bin  $\log(M_{\text{star}}/M_{\odot}) = [10.5 - 11]$ . For the most massive galaxies considered,  $\sim 70$  per cent of the central galaxies are already passive. We can therefore distinguish two galaxy stellar mass regimes:

- (i) an *satellite quenching dominated* regime: galaxies with  $\log(M_{\text{star}}/M_{\odot}) < 10.5$  had their star formation rate mainly suppressed by the environment. Our results show that the estimated fractions of passive galaxies in this mass regime are in quite good agreement with the expected fraction of galaxies that have spent more than  $\sim 5 - 7$  Gyr in haloes more massive than  $10^{13} M_{\odot}$ ;
- (ii) a *central quenching dominated* regime: galaxies with  $\log(M_{\text{star}}/M_{\odot}) > 10.5$  whose star formation rate has been

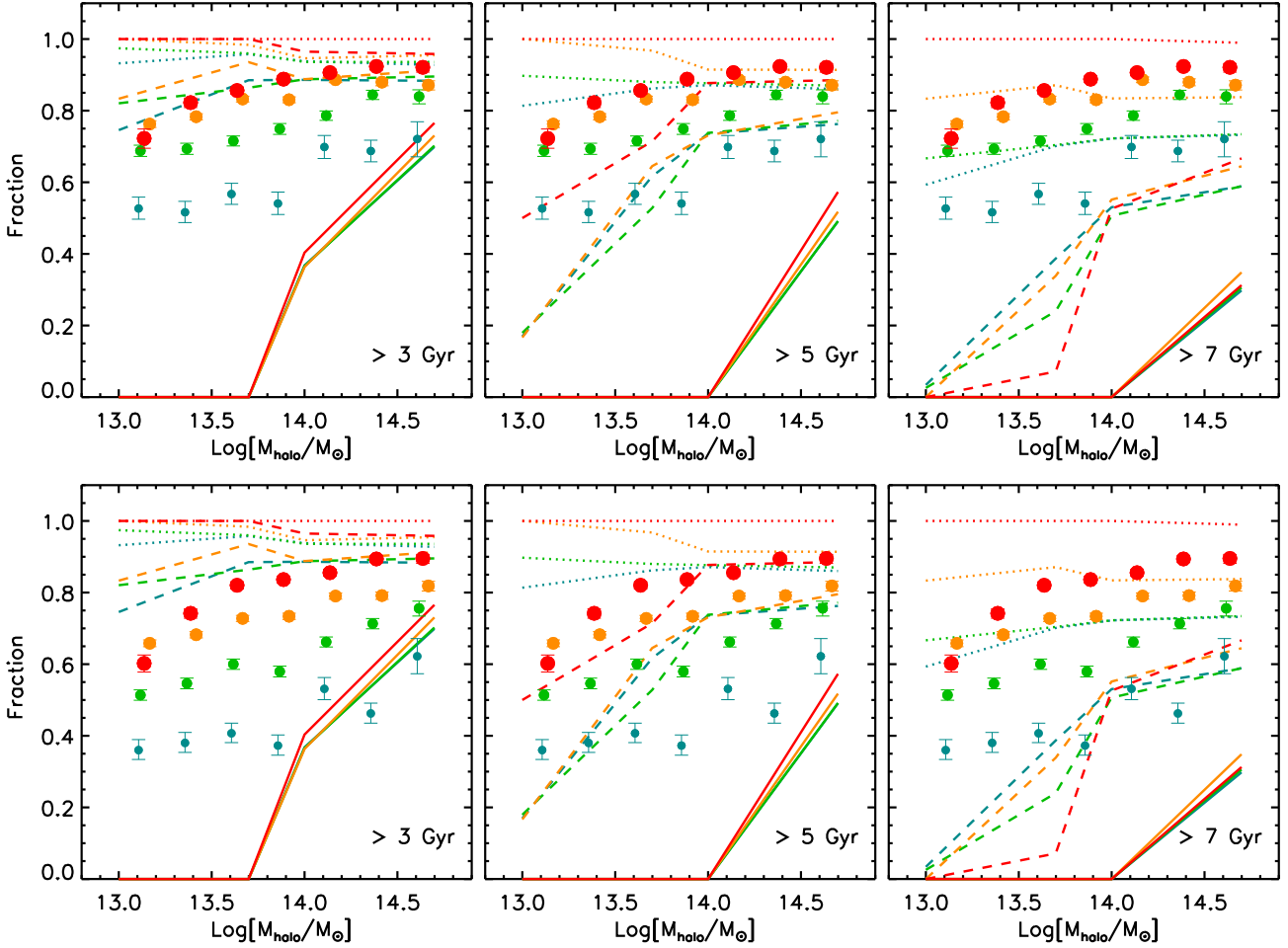


**Figure 11.** Fraction of model galaxies that spent more than 3 (left panel), 5 (middle panel), and 7 Gyr (right panel) in haloes more massive than  $10^{12}$  (dotted lines),  $10^{13}$  (dashed lines), and  $10^{14} M_{\odot}$  (solid lines). Fractions are plotted as a function of the present day halo mass. Different colours correspond to different galaxy stellar mass bins: cyan corresponds to  $\log(M_{\text{star}}/M_{\odot}) = [9.5 - 10]$ , green to  $\log(M_{\text{star}}/M_{\odot}) = [10 - 10.5]$ , orange to  $\log(M_{\text{star}}/M_{\odot}) = [10.5 - 11]$ , and red to  $\log(M_{\text{star}}/M_{\odot}) = [11 - 12]$ . Data points with error bars are observational estimates of red fractions (top panels) and passive fractions (bottom panels) based on the DR4 catalogue by Yang et al. (2007). Error bars denote confidence intervals from quartiles of the beta distribution.

reduced primarily by internal physical processes. For these galaxies, the estimated passive fractions shown in Figure 11 favour a somewhat lower value of  $T_{\text{halo}} \sim 5$  Gyr. This could be due to the fact that these galaxies have spent some fraction of their lifetime as central galaxies.

In order to determine the importance of environmental processes in suppressing the star formation rates of satellite galaxies, we follow van den Bosch et al. (2008) and define the following *transition fraction*:

$$\text{frac}_{\text{env}} = \frac{\text{frac}_{\text{red,sat}} - \text{frac}_{\text{red,cen}}}{\text{frac}_{\text{blue,cen}}} \quad (2)$$

where  $\text{frac}_{\text{red,sat}}$  is the fraction of satellite galaxies that are red,  $\text{frac}_{\text{red,cen}}$  is the fraction of central galaxies that are red, and  $\text{frac}_{\text{blue,cen}}$  is the fraction of central galaxies that are blue. As discussed by van den Bosch et al. (2008), under the assumption that the present day population of central galaxies is representative of the progenitors of present-day satellite galaxies of the same stellar mass, the numerator of Eq. 2

gives the fraction of all satellite galaxies that have undergone a blue-to-red transition after their accretion. Dividing by the fraction of central galaxies that are blue, one obtains an estimate of the fraction of galaxies that turned red after they became satellite galaxies (i.e. because of the environmental quenching). An equivalent quantity can be defined using the measured fractions of passive and active satellite and central galaxies. In their study, van den Bosch et al. (2008) find that satellite quenching affects roughly 40 per cent of all galaxies that are still blue at the time of accretion, independently of their stellar mass.

Our results are shown in the top panel of Figure 12, and are compared to the same theoretical predictions that are given in Figure 11. Top panels show the red transition fractions (Eq. 2), while bottom panels show the corresponding measurements for passive fractions. As the errors on the transition fractions are dominated by the errors on the fraction of red/passive satellites, we have shown here the same error bars used in Figure 11. Both our red and passive transition fractions increase as a function of halo mass. A similar

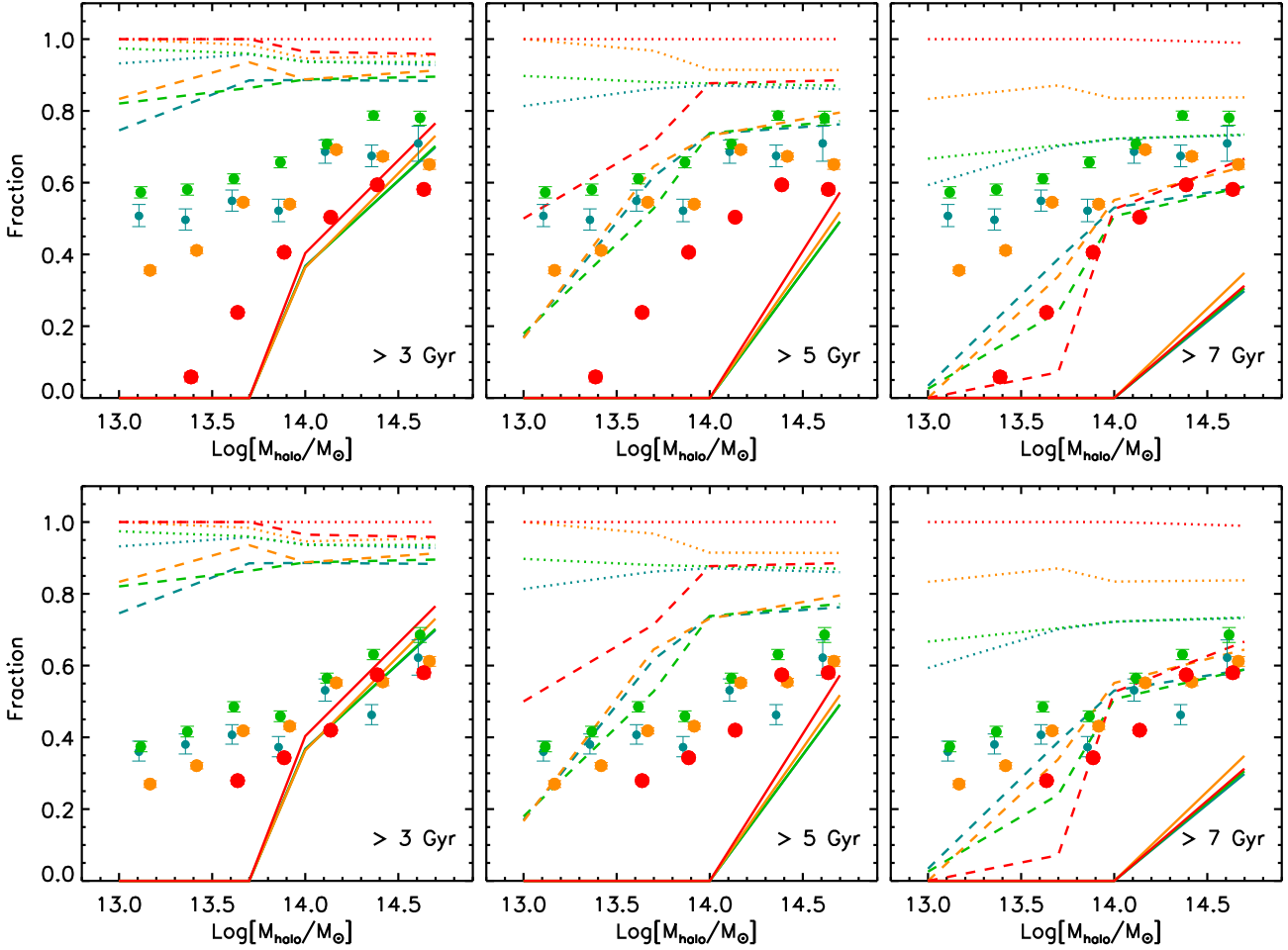


**Figure 12.** Lines show the same theoretical predictions given in Figure 11. Data points with error bars show the red (top panels) and passive (bottom panels) transition fractions, i.e. an estimate of the fractions of satellites that have been quenched by the environment (see text for details).

trend was recently found by Peng et al. (2011) who used, however, local overdensity as a proxy for the environment. The red transition fraction also shows a clear dependency as a function of the galaxy stellar mass: for the two lowest mass bins considered, the red transition fractions increase from  $\sim 55$  per cent in haloes of mass  $\sim 10^{13} M_{\odot}$  to  $\sim 75$  per cent in the most massive haloes considered in our sample ( $\sim 5 \times 10^{14} M_{\odot}$ ). For the most massive galaxies considered, no galaxy has been affected by environmental quenching in the lowest halo mass in our sample, while the transition fraction increases to  $\sim 60$  per cent in the most massive haloes considered. The passive transition fractions are offset low with respect to the corresponding red fractions except for the highest stellar mass bin, and the dependency on stellar mass is weaker. On average, the passive transition fractions vary between  $\sim 30$  per cent in the lowest mass haloes in our sample to  $\sim 65$  per cent in the most massive haloes. For haloes more massive than  $8 \times 10^{13} M_{\odot}$ , the estimated passive transition fractions follow quite nicely the trend expected for galaxies that spent more than  $\sim 7$  Gyr in haloes more massive than  $10^{13} M_{\odot}$ . For lower mass haloes, the figure favours a value of  $T_{\text{halo}}$  intermediate between 5 and 7 Gyr.

## 5 DISCUSSION

In the previous sections, we have characterized the *environmental history* of group and cluster galaxies. In particular, we have related the observed fractions of passive/red galaxies to the fraction of galaxies that have spent more than a given time ( $T_{\text{halo}}$ ) in a halo with mass larger than a given threshold ( $M_{\text{halo}}$ ). In this section, we discuss the main caveats of our analysis, and the main implications of our findings.

### 5.1 Caveats

As mentioned in Section 2, the galaxy formation model used in this study over-predicts the number of low to intermediate stellar mass galaxies. In particular, Guo et al. (2011) showed that the model used here over-predicts the number of galaxies in the stellar mass bin  $\log(M_{\text{star}}/M_{\odot}) = [9 - 10]$  by a factor  $\sim 2$ . For larger stellar masses, the model reproduces quite nicely the observed galaxy stellar mass function, as well as the halo occupation distribution measured for galaxy clusters both in the local Universe and at higher redshift

(Poggianti et al. 2010, but see also Liu et al. 2010)<sup>5</sup>. If the excess measured in the stellar mass bin  $\log(M_{\text{star}}/M_{\odot}) = [9 - 10]$  is due to galaxies that should have been stripped and/or merged with the central galaxy of their own parent halo, then there is likely an excess of galaxies with long survival times as satellites. Since we base our analysis on the *fraction* of galaxies that spent more than a given time in haloes more massive than some threshold, our predictions for this mass range should not be significantly affected.

We stress that our results are valid ‘on average’. As discussed above, there is a relatively large halo-to-halo variance that contributes, at least in part, to the scatter in the observed measurements. In addition, one should note that environmental effects very likely happen in a ‘probabilistic way’: not all satellites will continue forming stars for some given time and then simultaneously shut off. Otherwise, we would not observe a bimodality in the distribution of specific star formation rates. In reality, there will be satellite galaxies whose star formation rate will be suppressed on relatively short time-scales and other satellites that will maintain some level of star formation activity for longer times. This is probably in part related to the infalling orbital distribution of the satellite galaxies, as the orbital parameters will influence their dynamical friction timescale. McGee et al. (2009) argued that this should not affect significantly the results obtained if quenching requires relatively long time-scales, as those suggested by our study. The argument is based on the relatively narrow distribution of times that infalling dark matter substructures take to reach their pericentres from the virial radius (Benson 2005, see also Wetzel 2011). It should be noted, however, that the evolution of galaxies infalling onto larger haloes depends on other factors than their orbits, for example on the initial inclination of the discs with respect to their orbital planes (e.g. Villalobos et al. 2012), and variation in the inter-galactic medium properties of the host. Detailed numerical simulations are therefore needed to quantify the probability that a galaxy that has been orbiting within a halo of given mass has its star formation rate suppressed below some given threshold. As discussed above, our results suggest that the probability to be quenched approaches unity for galaxies that have spent 5 – 7 Gyr in haloes more massive than  $10^{13} M_{\odot}$ . These results might be useful in guiding the construction of halo occupation distribution models based on abundance matching for passive and active galaxies.

In Section 4, we have measured the red and passive transition fractions following van den Bosch et al. (2008), and assumed that the present-day population of central galaxies can be considered representative of the progenitors of present day satellite galaxies. As discussed in van den Bosch et al. (2008), this assumption is subject to a number of caveats. In particular: (i) in reality, one should consider the population of central galaxies at the average time of accretion of the satellite galaxy population; and (ii) the stellar mass of satellite galaxies might increase if they continue forming stars after accretion, and might decrease

because of tidal stripping. van den Bosch et al. (2008) argue that the cumulative effect should be small. We stress, however, that satellite galaxies in our model have been accreted over a wide range of cosmic epochs (see top left panel of Figure 7), and that the observed passive fractions require relatively long time-scales for the transition from blue/active to red/passive to occur. Therefore, the systematic errors on the transition fractions estimated in Section 3 could be relatively large.

## 5.2 What is the role of pre-processing?

In hierarchical cosmogonies, galaxy clusters are assembled through the accretion of lower mass haloes. Cluster galaxies might have resided for some time in ‘groups’, making *pre-processing* in these systems a potentially important phase for their evolution (Zabludoff & Mulchaey 1998). This has been discussed recently in two different studies that have used results from *N*-body simulations to analyse the accretion histories of cluster galaxies (Berrier et al. 2009; McGee et al. 2009). The conclusions obtained by these studies are quite different: Berrier et al. estimate that  $\sim 10$  per cent of the galaxies residing today in haloes of mass  $\sim 10^{14} M_{\odot}$  were accreted onto the cluster potential when residing in haloes more massive than  $10^{13} M_{\odot}$  (see their figure 2), and argue that pre-processing in a group environment is “of secondary importance for setting cluster galaxy properties for most clusters”. McGee et al. estimate, for clusters of similar mass, that about  $\sim 28$  per cent of the cluster galaxies have been accreted from haloes more massive than  $10^{13} M_{\odot}$  (see their figure 2). They also show that this fraction increases to  $\sim 45$  per cent for the most massive clusters in their sample, arguing that pre-processing in group environments “may be significant”.

The reason for this discrepancy lies mainly in the adoption of two different events corresponding to *accretion onto the cluster*. Berrier et al. (2009) use *N*-body simulations of galaxy clusters (with resolution similar to that of the Millennium Simulation used in this study), and assume that all bound substructures whose mass at the time of accretion is larger than some specific threshold, host a galaxy at their centre. By construction, the time used in Berrier et al. corresponds to our  $t_{\text{sat}}$ , i.e. the time when a galaxy first becomes satellite of a larger halo. McGee et al. (2009) use an approach that is equivalent to ours but base their analysis of a different semi-analytic model. Similarly to what we do, they trace the most massive progenitor of each galaxy back in time and record the halo mass of this progenitor at the time-step just before “the galaxy becomes a member of the final cluster”, which should correspond to our  $t_{\text{halo}}$ . We note that McGee et al. (2009) did not distinguish between galaxies that are accreted onto the final cluster as centrals, and those that are accreted as satellites. Both studies assume that a cluster galaxy was ‘pre-processed’ if it spent some (significant) fraction of its lifetime in a ‘group’ halo with mass  $\sim 10^{13} M_{\odot}$  before ‘being accreted onto the cluster’, independently of whether the galaxy is a central or a satellite.

As discussed above, the adoption of different characteristic times can lead to significantly different results, that also depend on the galaxy stellar mass. Considering only the haloes with mass  $\sim 10^{14} M_{\odot}$  in our sample, we find

<sup>5</sup> Note that Poggianti et al. (2010) used a magnitude limited sample both in their observational and model catalogues. We have verified that their magnitude limit corresponds approximately to a stellar mass limit of  $\sim 10^{10} M_{\odot}$ .



that only  $\sim 1$  per cent of the galaxies with stellar mass larger than  $10^9 M_\odot$  became satellites when residing in haloes more massive than  $\sim 10^{13} M_\odot$ . The fraction increases to  $\sim 4$  per cent when considering galaxies more massive than  $\sim 10^{10} M_\odot$ , and becomes  $\sim 37$  per cent when considering the most massive galaxies in the sample (those with stellar mass larger than  $\sim 10^{11} M_\odot$ ). Indeed, as we have discussed in Section 3, a larger fraction of these massive galaxies are accreted directly onto the final cluster as centrals. When considering the time when the galaxy is accreted onto the main progenitor of the cluster, we find that for the same haloes  $\sim 28$ ,  $\sim 29$ , and  $\sim 44$  per cent of galaxies with stellar mass larger than  $\sim 10^9$ ,  $\sim 10^{10}$  and  $\sim 10^{11} M_\odot$  were accreted from haloes more massive than  $\sim 10^{13} M_\odot$ . Our results are therefore in very good agreement with those found by McGee et al. (2009). An accurate comparison with results from Berrier et al. (2009) is complicated by the use of a different approach that does not trace directly the evolution of the galaxy stellar mass. Their primary cluster sample contains about 16 galaxies per cluster, which in our case would correspond to a galaxy stellar mass limit of  $\sim 2.6 \times 10^{10} M_\odot$ . Considering the fractions estimated above, our results are therefore not inconsistent with those obtained by Berrier et al. (2009).

If we define as pre-processed all galaxies that have spent time as satellites of a lower mass system before becoming part of a cluster<sup>6</sup>, our results show that the fraction of galaxies that can be pre-processed in a group-size halo of mass  $\sim 10^{13} M_\odot$  is significant. This fraction is largest for lowest mass galaxies. As discussed above, while  $\sim 44$  per cent of the most massive galaxies have been accreted from haloes more massive than  $\sim 10^{13} M_\odot$ , a large fraction of those have been accreted as centrals. On the other hand, basically all the  $\sim 28$  per cent low and intermediate mass galaxies that have been accreted from haloes more massive than  $\sim 10^{13} M_\odot$  are satellites at the time of accretion.

We stress that these results are natural consequences of hierarchical structure formation, and that they do not depend significantly on the particular semi-analytic model that we have used in our study. In order to understand how this preprocessing can affect the observed morphology-density relation, morphological mix, etc. it is therefore crucial to study the relevance and effects of various physical processes, at the scales typical of galaxy groups (specifically, halo masses  $\sim 10^{13} M_\odot$ ). Published numerical work on the role of environment on galaxy evolution, however, has so far focused largely on massive galaxy clusters, with very few numerical studies devoted to understand the effect of the group environment. Further numerical work in this direction is clearly needed (see e.g. Villalobos et al. 2012).

<sup>6</sup> We stress that this definition differs from that adopted in some earlier studies, including Berrier et al. (2009) McGee et al. (2009), who did not distinguish between physical processes acting only on satellite galaxies and processes that can affect all galaxies in a group.

### 5.3 Environment and time-scale of galaxy transformations

It has long been known that the local galaxy population consists roughly of two different types of galaxies: red galaxies with low levels of ongoing star formation and blue galaxies with active star formation. This *bimodality* is known to extend at least up to  $z \sim 1$  or higher (Bell et al. 2004; Whitaker et al. 2011), and to depend on the environment (e.g. Baldry et al. 2006). The physical origin of the observed bimodal distribution remains a question to be answered. In particular, it is unclear what is the characteristic time-scale of the galaxy transformation from blue/active to red/passive, and if this transformation is associated with a particular environment.

In our study, we have used the group catalogue by Yang et al. (2007) complemented with a cluster catalogue (von der Linden et al. 2007), and have tried to constrain these processes using two observational constraints: how the fraction of passive galaxies varies as a function of halo mass, and how the same quantity varies as a function of cluster-centric distance. In order to estimate the efficiency of satellite quenching, we have used the same statistics discussed by van den Bosch et al. (2008). We have shown that the fraction of satellite galaxies that have been quenched by the environment increases as a function of halo mass, from  $\sim 30$  per cent in the lowest mass haloes in our sample to about  $\sim 65$  per cent in the most massive haloes considered. The dependency on stellar mass is not large, and it tends to decrease for increasing halo mass.

Our calculations show that these observational trends are naturally explained by the fact that a larger fraction of satellite galaxies have spent long times in relatively massive haloes. Therefore, a more efficient quenching in more massive haloes is not required. These considerations give little support to cluster-specific processes like ram-pressure as the main drivers for the observed trends. In addition, the comparison with our theoretical predictions show that satellite galaxies become passive after they have spent a time  $T_{\text{halo}} \sim 5 - 7$  Gyr in haloes more massive than  $M_{\text{halo}} \sim 10^{13} M_\odot$ .

Several previous studies have argued for relatively long timescales for satellite quenching. E.g. Balogh, Navarro & Morris (2000) study the origin of cluster-centric gradients in star formation rates and colours of rich clusters assuming they are built from the accretion of field galaxies, and argue for a gradual decline (over a timescale of a few Gyr) of the star formation rate of cluster galaxies after accretion. Wang et al. (2007) use a physically based halo occupation distribution model and the observed distribution of 4000 Å break strengths to constrain the star formation histories of central and satellite galaxies. They find that satellite galaxies have declining star formation rates, with average e-folding times  $\tau_s \sim 2.5$  Gyr, and no significant dependency on stellar mass. Kang & van den Bosch (2008) use a semi-analytic model of galaxy formation and the observed increase in the red fraction of satellite galaxies as a function of stellar mass. They argue that model results can be brought into good agreement with the observational data by decreasing the stripping efficiency of the hot gas reservoirs associated with galaxies being accreted onto a larger halo. In particular, they assume a constant stripping rate over a time-scale of  $\sim 3$  Gyr. Recently,

Wetzel, Tinker & Conroy (2011) have used a group catalogue based on SDSS DR7 and studied the distribution of SSFRs for satellite galaxies and its dependence on stellar mass, halo mass and halo-centric distance. The ‘persistent bimodality’ they find for satellite galaxies indicate that star formation in active satellites continues to evolve (as in active centrals) for several Gyr. Several other studies have argued for relatively long timescales for the suppression of the star formation rates in satellite galaxies (Finn et al. 2008; Weinmann et al. 2009; De Lucia et al. 2009; Simard et al. 2009; von der Linden et al. 2010; McGee et al. 2011).

As explained in Section 2, a gradual stripping of the hot gas reservoir has been advocated and assumed in many recent studies based on semi-analytic models (see e.g. Font et al. 2008; Weinmann et al. 2010; Guo et al. 2011). It is, however, unclear how such a gentle mode of strangulation could support cooling and star formation in satellite galaxies for several Gyr. More detailed numerical studies are desirable to understand if the main problem with satellite galaxies in semi-analytic models is related to a poor treatment of environmental processes, or if it signals a more fundamental problem with the treatment of star-formation and feedback for these galaxies.

## 6 CONCLUSIONS

We exploit publicly available catalogues from semi-analytic models to study the environmental history of group and cluster galaxies. In particular, we focused on haloes with  $M_{200} > 10^{13} M_{\odot}$ , carried out our analysis within a theoretical framework, using the halo mass ( $M_{200}$ ) as a proxy for the environment, and considered explicitly the dependency on galaxy stellar mass. Our analysis highlights a number of natural consequences of structure formation that are important to consider when interpreting observational data. In particular, we show that:

- On average, the surviving massive satellites within galaxy groups/clusters were accreted later than their less massive counterparts and they come from more massive haloes. The most massive galaxies tend to be accreted onto the main progenitor of their final group/cluster when they are central galaxies of their own haloes. Less massive group/cluster members become satellites over a wide range of redshifts, and about half of them are accreted onto the final group/cluster when they are already satellite galaxies.
- The mixing of galaxy populations is incomplete during cluster assembly, which establishes a correlation between the time a galaxy is accreted onto a more massive halo (i.e. it becomes a satellite galaxy) and its distance from the final cluster centre. The radial trend is weakest for the most massive galaxies because of efficient dynamical friction and the late formation times of massive haloes.

These trends can be considered as the result of a *history bias*, that represents an integral part of the hierarchical framework. According to the current paradigm for structure formation, dark matter collapses into haloes in a bottom-up fashion. Small systems form first and subsequently merge to form progressively larger systems. As structure grows, galaxies join more and more massive systems, therefore experiencing a variety of environments during their lifetime. In this

framework, where a galaxy resides today (or at any cosmic epoch) depends heavily on what its past history was. Our analysis demonstrates also that binning galaxies according to their stellar mass does not suffice to disentangle the role of nature and nurture because galaxies of different stellar mass have different environmental histories. So, for example, two galaxies of identical mass at some cosmic epoch can end up having different stellar masses if one of them falls onto a cluster and the other remains in a region of average density.

The traditional *nature versus nurture debate*, as well as the controversy regarding the primacy of *stellar mass versus environment*, represent then subtle issues regarding ‘correlations’ and ‘attribution’. It is, in principle, possible to separate nature vs nurture if they are correlated but physically uncoupled. However, our results demonstrate that the two are strongly and physically connected so that any attempt to separate them is ill posed and misguided. We stress that this does not mean that studying galaxy properties at fixed stellar mass but in different environments does not provide important information, as demonstrated by a number of recent studies, many of which are referred to in this work. Results, however, should be interpreted with care.

To understand and quantify how hierarchical structure formation affects the observed environmental trends, we considered two observational constraints: the dependence of the passive galaxy fraction on halo mass, and cluster-centric distance. We based our observational measurements on the group catalogue by Yang et al. (2007) and the cluster catalogue by von der Linden et al. (2007). We used up-to-date estimates of the star formation rate and stellar masses, and complemented the cluster data with observational data available for the Coma and Virgo cluster presented by Weinmann et al. (2011).

We find that significant fractions of group/cluster galaxies have been accreted onto their final halo as members of groups with mass  $\sim 10^{13} M_{\odot}$ . For the particular model used in our study, and considering all haloes in our sample, we find that this fraction is  $\sim 27$  per cent for galaxies with stellar mass  $\sim 10^9$  and  $\sim 10^{10} M_{\odot}$ , and increases to  $\sim 44$  per cent for galaxies with mass  $\sim 10^{11} M_{\odot}$ . We also find that  $\sim 48$ ,  $\sim 43$ , and  $\sim 23$  per cent of the galaxies in the same stellar mass bins are accreted onto the main progenitor of the final halo as satellite galaxies. Large fractions of group and cluster galaxies have therefore been ‘pre-processed’ as satellites of groups with mass  $\sim 10^{13} M_{\odot}$ . Since a large fraction of the most massive galaxies we see in clusters today have been accreted as centrals, they have been pre-processed the least.

Comparisons with observational data suggest that galaxies become passive only after they have spent  $T_{\text{halo}} \sim 5-7$  Gyr in haloes more massive than  $M_{\text{halo}} = 10^{13} M_{\odot}$ . The observational trends are naturally explained by the growth of the large scale structure with no need for a more efficient quenching in the most massive haloes. It is unclear how satellite galaxies can sustain significant levels of star formation for such long time-scales and if this can be achieved, within the framework of current semi-analytic models of galaxy formation, by simply relaxing the assumption of instantaneous stripping of the hot gas reservoir associated with galaxies when they are accreted. On the numerical side, very little work has been carried out to understand the im-

portance and effects of different physical processes at the velocity dispersions typical of the group environment. Further studies in this directions are needed.

In this study, we have limited the analysis to haloes selected at redshift zero. A more comprehensive analysis extending to higher redshifts is clearly desirable and will likely provide important constraints on the physical processes (and related time-scales) responsible for establishing the observed environmental trends. Finally, we stress that our study is based on theoretical definitions of environment. In future work, we plan to extend the analysis outside the virial radius of dark matter haloes, and to use environment definitions that are closer to those commonly adopted in observational studies (e.g. local density). We believe that such an analysis will provide important guidance in the interpretation of observational results in a cosmological context, and in the comparison of studies at different cosmic epochs and/or from different surveys.

## ACKNOWLEDGEMENTS

The Millennium Simulation databases used in this paper and the web application providing online access to them were constructed as part of the activities of the German Astrophysical Virtual Observatory. We are grateful to G. Lemson for help with the Millennium Database, and to Anna Pasquali for her help with the SDSS DR7 data. GDL acknowledges financial support from the European Research Council under the European Community's Seventh Framework Programme (FP7/2007-2013)/ERC grant agreement n. 202781. We acknowledge fruitful discussions with Stefano Borgani, Olga Cucciati, Michaela Hirschmann, Anna Pasquali, Alvaro Villalobos, Dave Wilmann, and Simon White.

This paper has been typeset from a  $\text{\LaTeX}$  file prepared by the author.

## REFERENCES

- Avila-Reese V., Colín P., Gottlöber S., Firmani C., Maulbetsch C., 2005, *ApJ*, 634, 51
- Baldry I. K., Balogh M. L., Bower R. G., Glazebrook K., Nichol R. C., Bamford S. P., Budavari T., 2006, *MNRAS*, 373, 469
- Balogh M., Eke V., Miller C., Lewis I., Bower R., Couch W., Nichol R., Bland-Hawthorn J., et al. 2004, *MNRAS*, 348, 1355
- Balogh M. L., McGee S. L., 2010, *MNRAS*, 402, L59
- Balogh M. L., Navarro J. F., Morris S. L., 2000, *ApJ*, 540, 113
- Bell E. F., Wolf C., Meisenheimer K., Rix H.-W., Borch A., Dye S., Kleinheinrich M., Wisotzki L., McIntosh D. H., 2004, *ApJ*, 608, 752
- Benson A. J., 2005, *MNRAS*, 358, 551
- Berrier J. C., Stewart K. R., Bullock J. S., Purcell C. W., Barton E. J., Wechsler R. H., 2009, *ApJ*, 690, 1292
- Brinchmann J., Charlot S., White S. D. M., Tremonti C., Kauffmann G., Heckman T., Brinkmann J., 2004, *MNRAS*, 351, 1151
- Brüggen M., De Lucia G., 2008, *MNRAS*, 383, 1336
- Butcher H., Oemler Jr. A., 1984, *ApJ*, 285, 426
- Cameron E., 2011, *PASA*, 28, 128
- Cooper M. C., Newman J. A., Croton D. J., Weiner B. J., Willmer C. N. A., Gerke B. F., Madgwick D. S., Faber S. M., Davis M., Coil A. L., Finkbeiner D. P., Guhathakurta P., Koo D. C., 2006, *MNRAS*, 370, 198
- Cucciati O., Iovino A., Marinoni C., Ilbert O., Bardelli S., Franzetti P., Le Fèvre O., Pollo A., et al. 2006, *A&A*, 458, 39
- De Lucia G., 2011, in Ferreras, I. and Pasquali, A. ed., *Environment and the Formation of Galaxies: 30 years later*. Springer-Verlag, Heidelberg, p. 203
- De Lucia G., Blaizot J., 2007, *MNRAS*, 375, 2
- De Lucia G., Fontanot F., Wilman D., 2012, *MNRAS*, 419, 1324
- De Lucia G., Poggianti B. M., Halliday C., Milvang-Jensen B., Noll S., Smail I., Zaritsky D., 2009, *MNRAS*, 400, 68
- Desai V., Dalcanton J. J., Aragón-Salamanca A., Jablonka P., Poggianti B., Gogarten S. M., Simard L., Milvang-Jensen B., Rudnick G., Zaritsky D., Clowe D., Halliday C., Pelló R., Saglia R., White S., 2007, *ApJ*, 660, 1151
- Dressler A., 1980, *ApJ*, 236, 351
- Farouki R., Shapiro S. L., 1981, *ApJ*, 243, 32
- Finn R. A., Balogh M. L., Zaritsky D., Miller C. J., Nichol R. C., 2008, *ApJ*, 679, 279
- Font A. S., Bower R. G., McCarthy I. G., Benson A. J., Frenk C. S., Helly J. C., Lacey C. G., Baugh C. M., Cole S., 2008, *MNRAS*, 389, 1619
- Fontanot F., De Lucia G., Monaco P., Somerville R. S., Santini P., 2009, *MNRAS*, 397, 1776
- Gao L., Springel V., White S. D. M., 2005, *MNRAS*, 363, L66
- Gao L., White S. D. M., Jenkins A., Stoehr F., Springel V., 2004, *MNRAS*, 355, 819
- Gunn J. E., Gott III J. R., 1972, *ApJ*, 176, 1
- Guo Q., White S., Boylan-Kolchin M., De Lucia G., Kauffmann G., Lemson G., Li C., Springel V., Weinmann S., 2011, *MNRAS*, 413, 101
- Hubble E., Humason M. L., 1931, *ApJ*, 74, 43
- Kang X., van den Bosch F. C., 2008, *ApJ*, 676, L101
- Kauffmann G., Heckman T. M., White S. D. M., Charlot S., Tremonti C., Brinchmann J., Bruzual G., Peng E. W., et al. 2003, *MNRAS*, 341, 33
- Kauffmann G., White S. D. M., Heckman T. M., Ménard B., Brinchmann J., Charlot S., Tremonti C., Brinkmann J., 2004, *MNRAS*, 353, 713
- Kimm T., Somerville R. S., Yi S. K., van den Bosch F. C., Salim S., Fontanot F., Monaco P., Mo H., Pasquali A., Rich R. M., Yang X., 2009, *MNRAS*, 394, 1131
- Lemson G., Kauffmann G., 1999, *MNRAS*, 302, 111
- Li Y.-S., White S. D. M., 2008, *MNRAS*, 384, 1459
- Liu L., Yang X., Mo H. J., van den Bosch F. C., Springel V., 2010, *ApJ*, 712, 734
- Maulbetsch C., Avila-Reese V., Colín P., Gottlöber S., Khalatyan A., Steinmetz M., 2007, *ApJ*, 654, 53
- McCarthy I. G., Frenk C. S., Font A. S., Lacey C. G., Bower R. G., Mitchell N. L., Balogh M. L., Theuns T., 2008, *MNRAS*, 383, 593
- McGee S. L., Balogh M. L., Bower R. G., Font A. S., McCarthy I. G., 2009, *MNRAS*, 400, 937
- McGee S. L., Balogh M. L., Wilman D. J., Bower R. G.,

- Mulchaey J. S., Parker L. C., Oemler A., 2011, MNRAS, 413, 996
- Moore B., Lake G., Katz N., 1998, ApJ, 495, 139
- Oemler Jr. A., 1974, ApJ, 194, 1
- Peng Y., Lilly S. J., Renzini A., Carollo M., 2011, ApJ submitted, preprint (arXiv/1106.2546)
- Percival W. J., Scott D., Peacock J. A., Dunlop J. S., 2003, MNRAS, 338, L31
- Poggianti B. M., De Lucia G., Varela J., Aragon-Salamanca A., Finn R., Desai V., von der Linden A., White S. D. M., 2010, MNRAS, 405, 995
- Poggianti B. M., von der Linden A., De Lucia G., Desai V., Simard L., Halliday C., Aragón-Salamanca A., Bower R., et al. 2006, ApJ, 642, 188
- Saro A., De Lucia G., Borgani S., Dolag K., 2010, MNRAS, 406, 729
- Simard L., Clowe D., Desai V., Dalcanton J. J., von der Linden A., Poggianti B. M., White S. D. M., Aragón-Salamanca A., et al. 2009, A&A, 508, 1141
- Smith R. J., Lucey J. R., Price J., Hudson M. J., Phillipps S., 2012, MNRAS, 419, 3167
- Springel V., White S. D. M., Jenkins A., Frenk C. S., Yoshida N., Gao L., Navarro J., Thacker R., Croton D., Helly J., Peacock J. A., Cole S., Thomas P., Couchman H., Evrard A., Colberg J., Pearce F., 2005, Nature, 435, 629
- van den Bosch F. C., Aquino D., Yang X., Mo H. J., Pasquali A., McIntosh D. H., Weinmann S. M., Kang X., 2008, MNRAS, 387, 79
- Villalobos Á., De Lucia G., Borgani S., Murante G., 2012, MNRAS in press, arXiv/1202.0550
- von der Linden A., Best P. N., Kauffmann G., White S. D. M., 2007, MNRAS, 379, 867
- von der Linden A., Wild V., Kauffmann G., White S. D. M., Weinmann S., 2010, MNRAS, 404, 1231
- Wang J., De Lucia G., Kitzbichler M. G., White S. D. M., 2008, MNRAS, 384, 1301
- Wang L., Li C., Kauffmann G., De Lucia G., 2007, MNRAS, 377, 1419
- Wang L., Weinmann S. M., Neistein E., 2011, MNRAS in press, preprint (arXiv/1107.4419)
- Weinmann S. M., Kauffmann G., van den Bosch F. C., Pasquali A., McIntosh D. H., Mo H., Yang X., Guo Y., 2009, MNRAS, 394, 1213
- Weinmann S. M., Kauffmann G., von der Linden A., De Lucia G., 2010, MNRAS, 406, 2249
- Weinmann S. M., Lisker T., Guo Q., Meyer H. T., Janz J., 2011, MNRAS, 416, 1197
- Weinmann S. M., van den Bosch F. C., Pasquali A., 2011, in Ferreras, I. and Pasquali, A. ed., Environment and the Formation of Galaxies: 30 years later. Springer-Verlag, Heidelberg, p. 29
- Weinmann S. M., van den Bosch F. C., Yang X., Mo H. J., 2006, MNRAS, 366, 2
- Weinmann S. M., van den Bosch F. C., Yang X., Mo H. J., Croton D. J., Moore B., 2006, MNRAS, 372, 1161
- Wetzel A. R., 2011, MNRAS, 412, 49
- Wetzel A. R., Tinker J. L., Conroy C., 2011, MNRAS submitted, preprint (arXiv/1107.5311)
- Whitaker K. E., Labbé I., van Dokkum P. G., Brammer G., Kriek M., Marchesini D., Quadri R. F., Franx M., Muzzin A., Williams R. J., Bezanson R., Illingworth G. D., Lee K.-S., Lundgren B., Nelson E. J., Rudnick G., Tal T., Wake D. A., 2011, ApJ, 735, 86
- Wolf C., Aragón-Salamanca A., Balogh M., Barden M., Bell E. F., Gray M. E., Peng C. Y., Bacon D., et al. 2009, MNRAS, 393, 1302
- Yang X., Mo H. J., van den Bosch F. C., Pasquali A., Li C., Barden M., 2007, ApJ, 671, 153
- Zabludoff A. I., Mulchaey J. S., 1998, ApJ, 496, 39
- Zibetti S., Charlot S., Rix H.-W., 2009, MNRAS, 400, 1181